Corticospinal Tract Integrity in Acute Intracerebral Hemorrhage

by

Rebecca Clare McCourt

A thesis submitted in partial fulfillment of the requirements for the degree of

Master of Science

Centre for Neuroscience
University of Alberta

Thesis Abstract

Background: Intracerebral Hemorrhage (ICH) is associated with high morbidity and patients commonly suffer motor dysfunction. ICH volume is a significant predictor of outcome, and perihematoma edema may also represent tissue injury. Diffusion Tensor Imaging (DTI) can be used to assess in-vivo changes in tissue microstructure in white matter tracts, such as the Corticospinal Tract (CST). Using DTI, the deleterious effects of the hematoma and perihematoma edema on CST integrity and motor outcome may be assessed.

Methods: Patients with primary ICH underwent DTI at 72h, and days 7 and 30 after symptom onset. Diffusion metrics including Fractional Anisotropy (FA), a diffusion-based correlate for white matter integrity, were measured through the entire CST. Diffusion was also measured in the region of the ipsilateral CST that passed through the edema.

Results: DTI demonstrates evidence of impairment in the CST after ICH. Larger hematoma volumes were associated with lower FA values at day 30 (β= -0.77; p=0.003). FA was decreased in the CST where it passes through the edema, but was not related to motor outcome.

Conclusions: This study provides insight into the mechanisms of functional disability following hemorrhagic stroke. Hematoma volume is a mediating factor in white matter change after ICH, but diffusion changes in the perihematoma edema do not appear to be related to tract impairment.

Preface

This thesis is an original work by Rebecca McCourt. The research projects, of which this thesis is a part, received research ethics approval from the University of Alberta Research Ethics Board: "Intracerebral Hemorrhage Acutely Decreasing Arterial Pressure Trial II", No. 25022, August 31, 2011 and "Transient Ischemic Attack (TIA), Mild Ischemic and Intracerebral Hemorrhage Stroke Outcome Study", No. 00573, May 5 2009.

Dedication

To my family, whose love and support has been with me every step of the way.

Acknowledgements

I would like to thank my supervisor, Ken Butcher, who has been an exceptional guide and mentor to me over the past 5 years. I am truly grateful for his encouragement, support, and continual kindness and patience.

I owe a great debt of gratitude to my committee members, Dr. Richard Camicioli and Dr. Christian Beaulieu for providing advice and assistance in all aspects of my research.

I am so thankful to Dr. Sarah Treit for her insightful and intelligent assistance on this project, and for being an unfailingly friendly face; and to my fellow student Ehsan Misagi for providing crucial aspects of the imaging analysis.

I have benefitted from being part of a phenomenally friendly and supportive lab group, and want to thank all of the students and staff who were my companions in research. Leka Sivakumar deserves a special thank you for her invaluable ability to keep the lab running smoothly, and for her friendship.

I also owe thanks to the staff of the Neurology department who helped me with the administrative aspects of my graduate experience. A number of staff and students from the Centre for Neuroscience have made this journey so much more enjoyable by their presence, and special thanks go to the invaluable Megan Airmet. Finally, I would like to thank the physicians and nurses at the University of Alberta Hospital, and the members of the Peter Allen MR Centre who made my graduate project possible by enrolling and imaging patients.

Table of Contents

List of Tables

List of Figures

Chapter 1: Introduction to Intracerebral Hemorrhage

Intracerebral Hemorrhage

Primary Hemorrhage

Intracerebral hemorrhage (ICH) occurs when a blood vessel in the brain ruptures and blood enters the parenchyma. 10-20 %[1,2] of strokes are hemorrhagic, making it the second most common type after ischemic stroke.[3] ICH is classified as primary or secondary based on whether initiation of the bleed is spontaneous or non-spontaneous, respectively. The majority of this review will focus on primary ICH.

Primary ICH is the most common type of ICH (78-88%)[4,5] and describes the spontaneous rupture of vessels that have reduced integrity due to chronic hypertension/lipohyalinosis or cerebral amyloid angiopathy (CAA).[6] Primary ICH occurs more often in some locations of the brain than others. Basal ganglia bleeds are the most common (44%-74%)[2,5,7] and are associated with a history of hypertension.[4] Lobar bleeds are the second most common, occurring in 26-45%[2,7] of cases, and are associated with CAA. Other locations of ICH include the thalamus (15-25%),[5] brainstem (3-6%),[2,7] and cerebellum (6%).[2] Epidural and subdural hemorrhages are usually secondary to head trauma. Subarachnoid hemorrhage location is often associated with aneurysms.[8]

Secondary Hemorrhage

Secondary or non-spontaneous hemorrhage may arise from vascular malformations (primarily arteriovenous and cavernous malformations), aneurysm, cerebral vein thrombosis, hereditary or acquired coagulopathies, or tumour.[6,8] Hematomas arising in the area of ischemic stroke infarction are referred to as hemorrhagic transformations. Anticoagulant-associated ICH

represents 12-20% of ICH patients, who tend to have larger bleeds and worse outcomes.[9] Anticoagulants do not cause ICH, but are commonly prescribed in patients with ICH risk factors, and the coagulopathy presents a complication to treatment.

Incidence of Primary Intracerebral Hemorrhage

Worldwide incidence of ICH is estimated to be 10-20 per 100,000.[6] A prospective, population based registry of 549 European ICH patients reported a similar incidence of 15.9 per 100,000.[2] A similar registry in Kerala, India assessed incidence for ICH as 10.1 per 100,000.[10] A very large meta-analysis of 36 studies of ICH incidence from 21 countries, spanning from 1980 to 2008 (n>8000), reported an incidence of 24.6 per 100,000 person-years.[11] They found that incidence did not change significantly during that time span. The same meta-analysis reported ethnicity-based differences in ICH incidence. Incidence (per 100,000 people years) was comparable between Caucasian (24.1) and black people (22.9), decreased in Hispanic individuals (19.6), and was nearly twice as high in East and Southeast Asian individuals (51.9).[11] Other studies have reported higher incidences of ICH of 50 per 100,000 in black people.[6] Incidence of ICH is higher in men,[2] and older individuals.[6]

Diagnosis of Intracerebral Hemorrhage

Symptoms

Patients with ICH often present with headache and vomiting.[9] Decreased level of consciousness is common (50% of cases), especially in larger ICH with compression of the brainstem.[6,8] ICH patients tend to present at admission with lower levels of consciousness than ischemic patients.[4] Other neurological symptoms include sensory-motor deficits secondary to damage of the basal ganglia and thalamus, gaze deviation and cranial nerve symptoms associated with brainstem

involvement, motor deficits resulting from cerebellar damage, and various cortical signs including aphasia and neglect.[6]

Diagnostic Imaging

Stroke diagnosis relies on imaging technology. Vomiting and headaches are more common in hemorrhagic than ischemic stroke,[8] and rough localization of the stroke is possible using neurological signs, but clinical imaging is required to confirm a diagnosis. CT scans are available in most emergency departments and are the gold standard for diagnosis of ICH.[9] MRI is not as commonly available as CT but is also effective for diagnosis of ICH,[9] particularly the T2-weighted and gradient-echo sequences.

Imaging is also used to differentiate primary and secondary etiology. For instance, CT- or MR-angiography can be helpful in identifying vascular abnormalities, while presence of a fluid-fluid level on acute CT suggests anti-coagulant associated hemorrhage.[5] Investigation of underlying primary causes is especially warranted in young patients without a history of hypertension.[9]

Risk Factors

Modifiable Risk Factors

Up to 60% of ICH cases are caused by high blood pressure.[12] The Stroke Data Bank, a study of outcome and prognosis in 1805 ICH patients, reported that 38-75% of patients had a history of hypertension.[4] The higher the blood pressure, the more increased the risk of hemorrhage; for example: systolic pressures between 140-159 mm Hg vs. pressure over 160 mm Hg were associated with 1.4 and 5.5 times the risk for ICH, respectively.[13]

In terms of diet and lifestyle-related risk factors, moderate to high alcohol intake,[14] smoking, lower levels of cholesterol and triglycerides,[13,14] and stimulant use[9] are associated with increased

risk of ICH. Diabetes is associated with an approximately doubled risk of ICH.[15] Lower level of education is also a risk factor, potentially related to lack of education on the aforementioned diet and lifestyle factors.[6]

History of previous stroke also increases risk of hemorrhage.[9] After ICH, estimates for recurrence for a second hemorrhage are up to 25%.[16] A Canadian retrospective review of 423 patients with stroke reported approximately equal risk of recurrent ICH vs. ischemic stroke (2.4% vs 3.0%, respectively).[16] CAA-associated lobar ICH was significantly associated with readmission for ICH.[16] Recurrent risk of hemorrhage is approximately 2% in hypertensive-related ICH and 10% in CAA-related ICH.[6]

Non-Modifiable Risk Factors

Increased age, particularly age over 55, is associated with ICH risk.[2] A longitudinal study of cardiovascular health in over 21,000 individuals found that the relative rate of ICH doubled with every decade.[13] Fatality is higher in patients older than 72 years (28% case fatalities) compared to patients younger than 72 (18% case fatalities).[11] CAA increases with age and is a contributing factor to the increased risk of ICH with age.[6] CAA is thought to be responsible for up to 50% of lobar hemorrhages.[15]

Male gender is associated with higher risk of ICH than female gender. A systematic review of 25 case-control and cohort ICH studies found a 3-4 time increase in risk in males compared to females.[14] However other studies report relatively lower risk rate between the genders (1.2-1.5 times increased risk for males).[13] Ethnicity is also a risk factor for ICH: a pooled analysis of two large prospective ICH studies in the United States found that being black was associated with

nearly twice the risk of ICH compared to Caucasians.[13] A retrospective Canadian study of ethnic variations in ICH found an approximately doubled presentation of East and South Asian patients compared to Caucasians.[17]

Prognosis

Death and Morbidity

ICH is associated with poor functional outcome and high mortality. ICH has a three-times increased risk of fatality within the first year compared to ischemic stroke.[2] 30-50% of patients die within 30 days of onset,[4,18] with the majority of mortality occurring within 24 hours.[19] Estimates of survival at 10 years vary from 24-30%.[2] ICH patients have more significant disability than ischemic patients.[20] ICH accounts for over 65 million disability-associated life years, making it a significant cause of disability worldwide[21]. Up to 80% of ICH survivors are unable to live independently 6 months after stroke.[22] Morbidity is often established early on, with around 65% of ICH patients reporting total dependence on functional scores at admission.[4]

Motor Impairment

The primary pathway controlling motor function in humans is the corticospinal tract (CST). The most common location for primary ICH, the basal ganglia, is immediately adjacent to the pathway of the CST through the internal capsule and brainstem.[7] Unsurprisingly, motor impairment after ICH is common. 61% of patients in a study of >200 were admitted with symptoms of hemiplegia after ICH,[7] and up to 60% of stroke survivors have motor impairments even after rehabilitation.[23] Mass effect, neurotoxic blood breakdown products, and inflammatory cascades damage the tissue surrounding the hematoma.[24] Experimental models demonstrate neuronal death and destruction of white matter projections in the region of the bleed,[25,26] and

Wallerian degeneration of the CST after ICH can be detected within 2 weeks of onset on MRI.[27,28]

Predictors of Outcome

The most significant predictor of outcome after ICH is hematoma volume (Figure 1.1). When combined with the Glasgow Coma Scale, ICH volume has a 96% sensitivity and 98% specificity for prediction of 30-day mortality.[19] In particular, ICH volumes over 60ml were associated with a 91% mortality at 30 days. ICH expansion is associated with worse outcome. Early ICH growth (≤48h) predicted clinical deterioration at 48 hours in a group of 266 ICH patients.[29] Expansion is exacerbated in patients with anticoagulant-associated ICH,[1] and these patients typically have worse outcomes. Expansion occurs in approximately 30% of patients within 1 hour of onset and within 20 hours in 50% of patients.[30]

Interventricular hemorrhage, or the extension of blood into the ventricles occurs in approximately 45% of cases[9] and is also associated with poor prognosis. In a study of over 200 patients with hemorrhage, 100% of patients with massive ventricular extension died within 24 hours.[7] Patients with high blood pressure at admission are at an increased risk of mortality.[6] Other independent predictors of survival include increased age and higher Glasgow Coma Scale.[18]

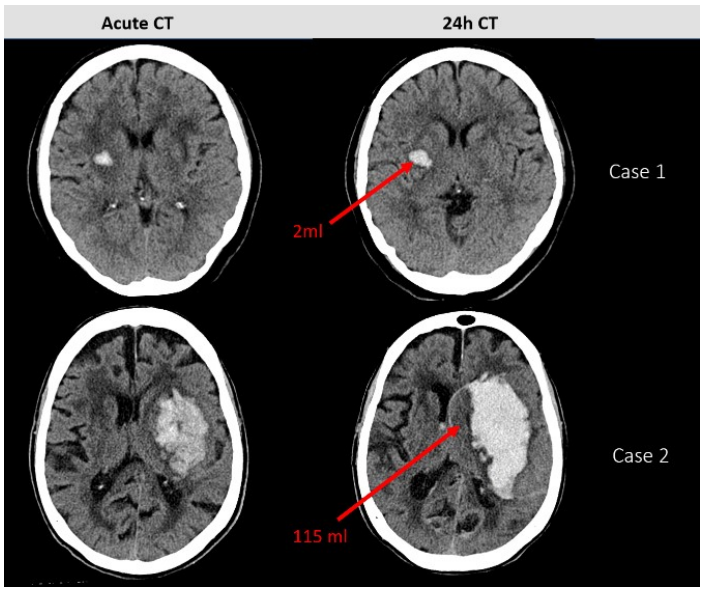

Figure 1.1. Example of Intracerebral Hemorrhage Volumes in Patients with Good vs. Poor Outcome. Case 1: a 59-year old woman developed left-sided weakness, facial droop, & slurred speech. Hematoma volume did not expand significantly and she had a good outcome with essentially no symptoms. Case 2: 77-year old woman with slurred speech, right-sided paralysis, and a large expanding hematoma. The patient died one week from onset.

Perihematoma Edema

Edema Etiology

Imaging signal changes observed in the region surrounding acute intracerebral hemorrhage are often referred to as perihematoma edema. Acutely, edema appears as a hyperintense ring surrounding the hematoma on FLAIR, and hypointense ring on CT. Etiology of perihematoma edema has been commonly attributed to plasma extrusion during clot contraction.[31–33] Vasogenic edema, or increased fluid movement from the intravascular to extravascular space, has also been postulated as a mechanism of edema formation.[31,34,35] Finally, observations of reduced blood

flow in the perihematoma region have led to the hypothesis that perihematoma edema is a result of secondary ischemic injury. In this case, reduced metabolic supply would cause failure of Na/K-ATPase pumps and resultant intracellular accumulation of water.[34,36] Cell swelling would follow and the tissue in this region would be endangered. For this reason, perihematoma edema is sometimes regarded as a marker of secondary hematoma injury. However, absolute reductions in perihematoma blood flow do not appear to be significant enough to result in ischemic injury in most cases.[37]

Prognostic Significance

Perihematoma edema volumes are reliably correlated with hematoma volume,[38,39] but prognostic relevance is uncertain. Studies correlating edema volumes with outcome have mixed results. Several studies found that edema was associated with poor outcome,[40–42] while others have reported no relationship.[43,44] One study even found that outcomes improve when relative edema volume is larger.[43]

Summary

ICH occurs when a blood vessel in the brain ruptures and blood enters the parenchyma. It is the second most common type of stroke and is associated with high mortality and morbidity. It primarily affects men and people of older age. Imaging is required to confirm diagnosis and there is no proven treatment. Prevention of ICH is based on avoiding modifiable risk factors such as hypertension. Motor dysfunction after ICH is common and contributes significantly to the extent of disability.

References

1. Asdaghi, N., Manawadu, D. & Butcher, K. Therapeutic management of acute intracerebral haemorrhage. *Expert Opin. Pharmacother.* **8,** 3097–116 (2007).
2. Sacco, S., Marini, C., Toni, D., Olivieri, L. & Carolei, A. Incidence and 10-year survival of intracerebral hemorrhage in a population-based registry. *Stroke.* **40,** 394–9 (2009).
3. Grysiewicz, R. A., Thomas, K. & Pandey, D. K. Epidemiology of ischemic and hemorrhagic stroke: incidence, prevalence, mortality, and risk factors. *Neurol. Clin.* **26,** 871–95, vii (2008).
4. Foulkes, M. A. & others. The Stroke Data Bank: design, methods, and baseline characteristics. *Stroke* **19,** 547–554 (1988).
5. Linn, J. & Brückmann, H. Differential diagnosis of nontraumatic intracerebral hemorrhage. *Klin. Neuroradiol.* **19,** 45–61 (2009).
6. Qureshi, A. I. *et al.* Spontaneous Intracerebral Hemorrhage. *NEJM* **344,** 1450–1460 (2001).
7. Mutlu, N., RG, B. & BJ, A. Massive cerebral hemorrhage: Clinical and pathological correlations. *Arch. Neurol.* **8,** 644–661 (1963).
8. Sahni, R. & Weinberger, J. Management of intracerebral hemorrhage. *VHRM* **3,** 701–709 (2007).
9. Hemphill, J. C. *et al.* Guidelines for the Management of Spontaneous Intracerebral Hemorrhage: A Guideline for Healthcare Professionals from the American Heart Association/American Stroke Association. *Stroke* **46,** (2015).
10. Sridharan, S. E. *et al.* Incidence, types, risk factors, and outcome of stroke in a developing country the trivandrum stroke registry. *Stroke* **40,** 1212–1218 (2009).

11. van Asch, C. J. *et al.* Incidence, case fatality, and functional outcome of intracerebral haemorrhage over time, according to age, sex, and ethnic origin: a systematic review and meta-analysis. *Lancet Neurol.* **9,** 167–76 (2010).

12. Magistris, F., Bazak, S. & Martin, J. Intracerebral Hemorrhage: Pathophysiology, Diagnosis and Management. *MUMJ* **10,** 15–22 (2000).

13. Sturgeon, J. D. *et al.* Risk factors for intracerebral hemorrhage in a pooled prospective study. *Stroke* **38,** 2718–2725 (2007).

14. Ariesen, M. J., Claus, S. P., Rinkel, G. J. E. & Algra, A. Risk factors for intracerebral hemorrhage in the general population: A systematic review. *Stroke* **34,** 2060–2065 (2003).

15. Ikram, M. A., Wieberdink, R. G. & Koudstaal, P. J. International epidemiology of intracerebral hemorrhage. *Curr. Atheroscler. Rep.* **14,** 300–6 (2012).

16. Hill, M. D., Silver, F. L., Austin, P. C. & Tu, J. V. Rate of stroke recurrence in patients with primary intracerebral hemorrhage. *Stroke.* **31,** 123–127 (2000).

17. Khan, N. a *et al.* Risk factors, quality of care and prognosis in South Asian, East Asian and White patients with stroke. *BMC Neurol.* **13,** 74 (2013).

18. Gebel, J. M. & Broderick, J. P. Intracerebral hemorrhage. *Neurol. Clin.* **18,** 419–38 (2000).

19. Broderick, J. P., Brott, T. G., Duldner, J. E., Tomsick, T. & Huster, G. Volume of intracerebral hemorrhage. A powerful and easy-to-use predictor of 30-day mortality. *Stroke.* **24,** 987–993 (1993).

20. Katrak, P. H., Black, D. & Peeva, V. Do stroke patients with intracerebral hemorrhage have a better functional outcome than patients with cerebral infarction? *PM & R* **1,** 427–33 (2009).

21. Krishnamurthi, R. V. *et al.* Global and regional burden of first-ever ischaemic and haemorrhagic stroke during 1990-2010: Findings from the Global Burden of Disease Study 2010. *Lancet Glob. Heal.* **1,** (2013).

22. Broderick, J. P. *et al.* Guidelines for the Management of Spontaneous Intracerebral Hemorrhage. *Stroke* **30,** 905–915 (2015).

23. Gor-Garcia-Fogeda, D. *et al.* Scales to assess gross motor function in stroke patients: A systematic review. *Arch. Phys. Med. Rehabil.* **95,** 1174–1183 (2014).

24. Xi, G., Keep, R. F. & Hoff, J. T. Mechanisms of brain injury after intracerebral haemorrhage. *Lancet Neurology* **5,** 53–63 (2006).

25. Barratt, H. E., Lanman, T. A. & Carmichael, S. T. Mouse intracerebral hemorrhage models produce different degrees of initial and delayed damage, axonal sprouting, and recovery. *J. Cereb. Blood Flow Metab.* **34,** 1463–71 (2014).

26. Wasserman, J. K. & Schlichter, L. C. White matter injury in young and aged rats after intracerebral hemorrhage. *Exp. Neurol.* **214,** 266–275 (2008).

27. Venkatasubramanian, C. *et al.* Natural history and prognostic value of corticospinal tract Wallerian degeneration in intracerebral hemorrhage. *JAHA* **2,** e000090 (2013).

28. Thomalla, G. *et al.* Diffusion tensor imaging detects early Wallerian degeneration of the pyramidal tract after ischemic stroke. *Neuroimage* **22,** 1767–1774 (2004).

29. Leira, R. *et al.* Early neurologic deterioration in intracerebral hemorrhage: predictors and associated factors. *Neurology* **63,** 461–7 (2004).

30. Brott, T. *et al.* Early hemorrhage growth in patients with intracerebral hemorrhage. *Stroke.* **28,** 1–5 (1997).

31. Wagner, K. R. *et al.* Lobar intracerebral hemorrhage model in pigs: rapid edema

development in perihematomal white matter. *Stroke.* **27,** 490–497 (1996).

32. Xi, G. *et al.* Role of Blood Clot Formation on Early Edema Development After Experimental Intracerebral Hemorrhage. *Stroke* **29,** 2580–2586 (1998).

33. Zazulia, A. R., Videen, T. O., Diringer, M. N. & Powers, W. J. Poor correlation between perihematomal MRI hyperintensity and brain swelling after intracerebral hemorrhage. *Neurocrit. Care* **15,** 436–41 (2011).

34. Xi, G., Keep, R. F. & Hoff, J. T. Pathophysiology of brain edema formation. *Neurosurg Clin N Am* **13,** 371–383 (2002).

35. Butcher, K. S. *et al.* Perihematomal edema in primary intracerebral hemorrhage is plasma derived. *Stroke* **35,** 1879–1885 (2004).

36. Olivot, J.-M. M. *et al.* MRI profile of the perihematomal region in acute intracerebral hemorrhage. *Stroke* **41,** 2681–2683 (2010).

37. Butcher, K. S. *et al.* The Intracerebral Hemorrhage Acutely Decreasing Arterial Pressure Trial. *Stroke.* **44,** 620–6 (2013).

38. Carhuapoma, J. R., Hanley, D. F., Banerjee, M. & Beauchamp, N. J. Brain edema after human cerebral hemorrhage: a magnetic resonance imaging volumetric analysis. *J. Neurosurg. Anesthesiol.* **15,** 230–3 (2003).

39. Carhuapoma, J. R., Barker, P. B., Hanley, D. F., Wang, P. & Beauchamp, N. J. Human Brain Hemorrhage : Quantification of Perihematoma Edema by Use of Diffusion-Weighted MR Imaging. *AJNR* **23,** 1322–1326 (2002).

40. Urday, S. *et al.* Hemorrhage. *Stroke* **46,** 1–11 (2015).

41. Murthy, S. B. *et al.* Perihematomal Edema and Functional Outcomes in Intracerebral Hemorrhage Influence of Hematoma Volume and Location. *Stroke* **46,** 1–12 (2015).

42. Fan, Y. & Lin, K. Changes in structural integrity are correlated with motor and functional recovery after post- stroke rehabilitation Changes in structural integrity are correlated with motor and functional recovery after post-stroke rehabilitation. *Rest. Neurol. and Neuro.* **33,** 835–844 (2015).

43. Gebel, J. M. *et al.* Relative Edema Volume Is a Predictor of Outcome in Patients With Hyperacute Spontaneous Intracerebral Hemorrhage. *Stroke* **33,** 2636–2641 (2002).

44. Arima, H. *et al.* Significance of perihematomal edema in acute intracerebral hemorrhage: the INTERACT trial. *Neurology* **73,** 1963–1968 (2009).

Chapter 2: Diffusion Tensor Imaging

Introduction

Effective stroke diagnosis and treatment relies on imaging technology. Magnetic Resonance Imaging (MRI), in addition to a use in stroke diagnosis, can be used to analyze post-stroke structural and functional changes in vivo. The development and refinement of imaging techniques like Diffusion Weighted Imaging (DWI) and its derivative, Diffusion Tensor Imaging (DTI), are essential to the improvement of prognosis, treatment, and outcome analysis in stroke.

DTI tracks the diffusion of water molecules in tissue, and can be used to indirectly assess white matter integrity. It has the promising ability to assess pathological tissue changes non-invasively and in vivo. The aim of this review is to provide a brief overview of DTI in order to understand the potential of its application to imaging of ICH.

Diffusion Imaging

The Diffusion Sequence

In conventional MR, tissue is differentiated based on varying relaxation times for hydrogen, following activation by a radiofrequency (RF) pulse.[1] In DWI, two diffusion-sensitizing magnetic gradients are applied in combination with the RF pulses, allowing water molecules to be differentiated based on their location in the brain, and the extent of their diffusion.

The intensity of the diffusion signal can be modified by controlling various aspects of the diffusion sequence, such as TE (echo time), TR (repetition of the MR signal), and *b*, the diffusion weighting factor.[2] The *b*-value determines the strength and length of gradient application such that a b=0 s/mm^2 image has no diffusion weighting and is essentially a reference

T2 image, while a *b*=1000 s/mm^2 delivers a highly diffusion-weighted image in which pathology is highly contrasted.[2] At least two b-values are used to create a diffusion map: one with a high b-value to provide diffusion weighting, and a second with no diffusion weighting, b=0 s/mm^2, to provide a baseline MR signal.[3] The diffusion coefficient can then be calculated based on the signal attenuation that occurs when water molecules move in the pause between the two diffusion-sensitizing gradients.[4] During a typical pause of 50 ms between gradients, the average water dispersion (usually about 10 μm) is influenced by the surrounding tissue structure.[5]

DTI is most frequently acquired using single-shot echo-planar imaging (EPI) sequences. EPI has the advantage of being fast, having good signal-to-noise ratio (SNR), and being relatively resilient to motion.[3] However, it has low spatial resolution and suffers from distortions at bone-air-brain interfaces due to magnetic field inhomogeneities.[3]

Assessing Diffusion Direction

In order to obtain information on the direction of diffusion, water displacement is measured in a minimum of six directions. Acquisition of more than six directions is desirable in order to maximize SNR and provide robust estimations of the diffusion tensor, particularly for utilization of diffusion tractography.[3]

A directional ellipsoid can be calculated for each voxel based on diffusion tensors.[5] The diffusion ellipsoid is described by three eigenvectors ($\varepsilon_1 - \varepsilon_3$) and three eigenvalues ($\lambda_1 - \lambda_3$) which represent the direction and amplitude of diffusion in the 3 primary directions of a voxel, respectively (Figure 2.1).[3]

When one eigenvalue has a larger magnitude than the others, the ellipsoid is cigar-shaped and indicates anisotropic diffusion in that voxel. The second and third eigenvectors are aligned

perpendicular to the primary eigenvector. When diffusion in a voxel is isotropic, as in the ventricles, then the diffusion ellipsoid is more spherical. This results in a set of directional data which can be used to describe fiber tracts and other architecture in the brain.

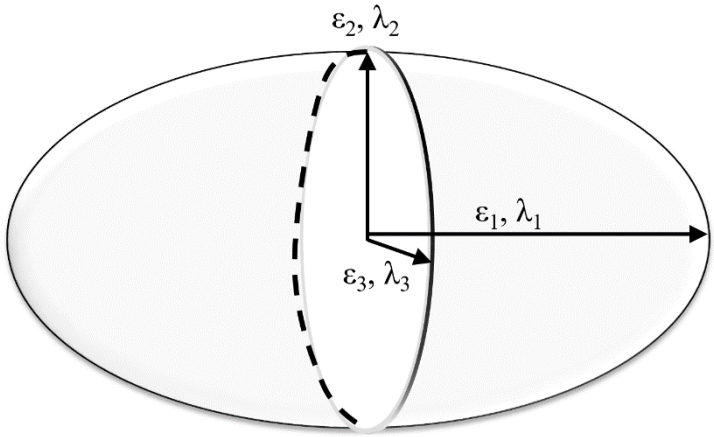

Figure 2.1 The Diffusion Ellipsoid. The directionality of diffusion in a voxel is described by three 'eigenvalues' (λ_1 –λ_3). The primary eigenvalue λ_1 aligns parallel to the main direction of diffusion, creating the cigar-shaped ellipsoid that is characteristic of anisotropic diffusion.

Diffusion Metrics

Fractional Anisotropy

Fractional anisotropy (FA) indicates the degree of anisotropy in tissue, described in a range of scalar values from completely isotropic (FA=0) to completely anisotropic (FA=1). FA varies with the aforementioned shape of the diffusion ellipsoid. As such, FA represents the type of diffusional movement within a voxel, which is a reflection of local microstructure (Figure 2.2). In white matter, the tightly organized neuronal bundles and their myelin sheaths promote directional diffusion.[6] FA values in white matter are higher than in grey matter, typically in the

range of 0.7-0.9 to 0.1-0.2, respectively.[5,7] FA decreases in white matter have been observed secondary to Wallerian degeneration.[8]

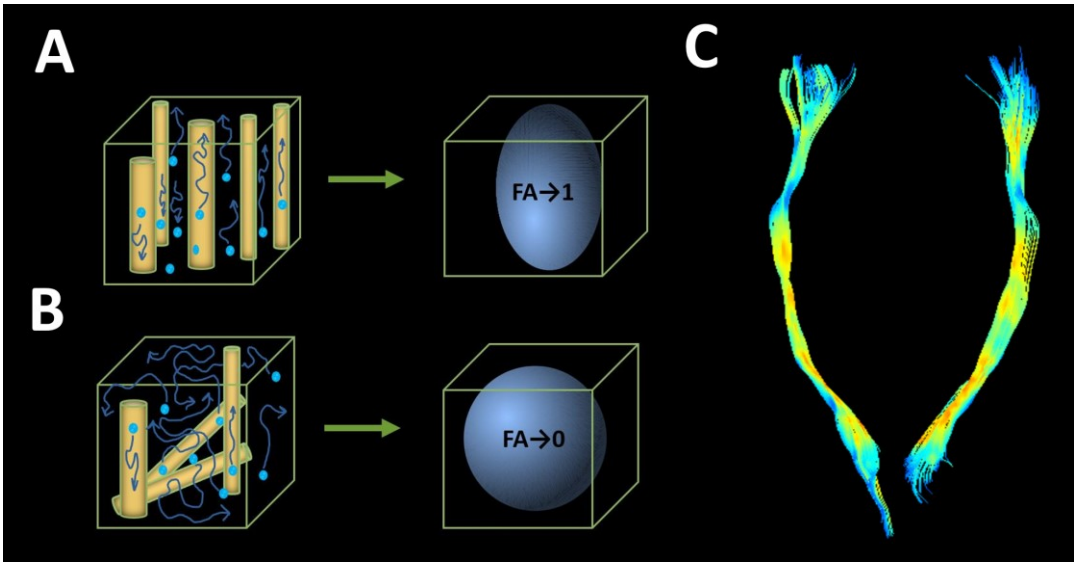

Figure 2.2. Fractional Anisotropy (FA) is a measure of diffusion directionality that reflects tissue microstructure. A) Diffusion directionality is increased in tissue with uniformly oriented structure, and FA values increase. B) Diffusion directionality is reduced in tissue with less organized structure, and FA values decrease. C) Three-dimensional model of a control corticospinal tract using diffusion tractography. Tracts are colour-coded by FA, with warmer colours indicating increased FA.

Mean Diffusivity

Mean Diffusivity (MD) is the average of λ_1-λ_3 and quantifies diffusion rate in units of mm^2/s.[3] MD is a scalar value and primarily reflects the extent of diffusion restriction. For instance, MD is decreased when diffusion is restricted by tissue boundaries, and increased in regions of unrestricted diffusion, such as the ventricles. MD is most commonly used to evaluate diffusion restriction secondary to injury in acute ischemic stroke.[4]

Axial and Radial Diffusion

Axial diffusion (AD) is equivalent to the primary eigenvector (λ_1), and describes diffusion along the main axis of the diffusion ellipsoid. In white matter, AD is thought to align parallel to tissue structures such as axonal bundles.[2] AD has been observed to decrease in animal models of spinal cord injury where axons are disrupted,[9,10] suggesting that it is influenced by axonal integrity.

Radial diffusion (RD) describes diffusion perpendicular to the main axes of the diffusion ellipsoid, and is calculated as the mean of (λ_2 and λ_3).[4] Increased RD has been observed in animal models of dysmyelination, suggesting that RD may reflect myelin integrity.[9,10] Together, AD and RD provide insight into changes in diffusion orientation that affect FA. FA values may be decreased as a result of RD increases, AD decreases, or both simultaneously.

A sample of diffusion maps for two patients with different volumes of ICH is shown in Figure 2.3.

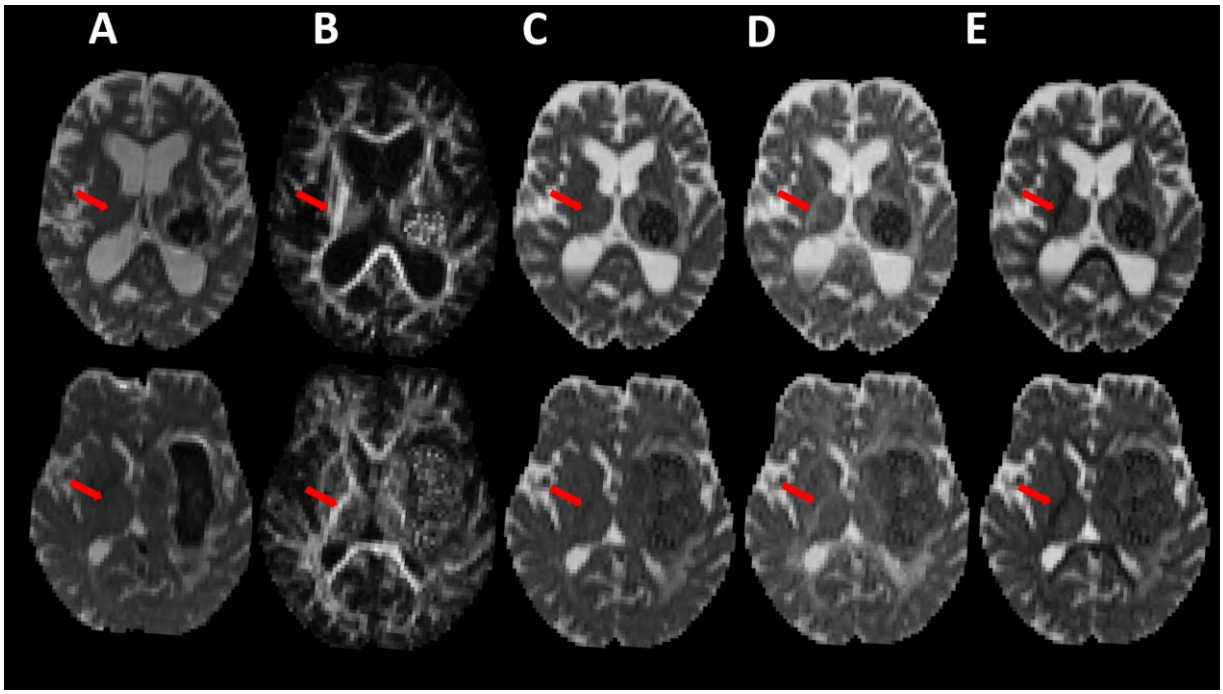

Figure 2.3. Diffusion maps at 48h post-hemorrhage in two patients. Top: A 69-year-old female with an 11.0 ml left thalamic hematoma. Bottom: An 81-year-old female with a 40.8 ml left basal ganglia hematoma. A) T2-weighted 'Mean of b=0 s/mm2' map showing hypo-intensity within the hematoma. B) Fractional Anisotropy map. Increased voxel intensity represents an increase in anisotropy and more directional diffusion. Note that the corticospinal tract (CST; red arrow), which contains highly oriented fibers, is hyperintense, indicating directional diffusion. C) Mean Diffusivity map. Increased intensity indicates increased rate of diffusion. Note that this map does not contain directional information, so white matter tracts are not as easily distinguished. D) Axial Diffusion map. Increased intensity indicates a larger magnitude of diffusion parallel to the axon, as shown in the CST. E) Radial Diffusion map. Increased intensity represents a larger magnitude of diffusion perpendicular to the axon. Note that the CST is hypointense.

Diffusion Tractography

Diffusion tensor information can be used to create three-dimensional maps of white matter tracts in the brain. The tracts may be colour-coded based on diffusion directionality or FA value along the tract (Figure 2.2C). DTT allows in-vivo assessment of three-dimensional tract damage, such as the identification of tract disruption in relation to the hematoma.[11] DTT has also recently been used to assess brain plasticity after ICH, adding to the understanding of the motor recovery process.[12]

Various algorithms may be used to produce diffusion tensor tractography results. In deterministic tractography, the algorithm starts at a selected region of interest (ROI) along the tract, then propagates along a path defined by the orientation of the vectors within adjoining voxels.[7] Propagation ends when the line enters a region of low anisotropy, often using a termination FA threshold of 0.2.[7] Probabilistic tractography propagates the tract based on a probabilistic estimation of connectivity.[13] Probabilistic tractography demonstrates better ability in differentiating regions of crossing fibers, whereas deterministic tractography is more reliable for the reproduction of long white matter tracts.[13]

Limitations of DTI

DTI voxel size is typically in the range of 2-3mm, allowing a voxel to contain numerous neuronal fibers.[2] This results in a number of limitations in DTI assessment of tracts.[5,7]

First, axonal relations within a single voxel cannot reliably be distinguished, which means that 'kissing' fibers (tracts that meet and separate without crossing) and crossing fibers look the same.[2] Secondly, deterministic tractography is limited when it comes to assessment of tracts with

multiple orientations, as several populations of neurons passing through the same voxel may simulate isotropic diffusion within that voxel. Regions of crossing fibers cause artificial anisotropy decreases in the voxel. Anisotropy values change depending on the orientation of the fibers (crossing vs. parallel bundles) so it is recommended that DTI results should be interpreted in the context of anatomical knowledge.[2] Noise can also cause inflation of anisotropy values.[3] Finally, any DTI measurement requiring the use of ROIs is naturally an operator-dependent method, and has associated error. The placement of the ROI can directly influence tractography results.[2]

It is also important to note that diffusion imaging provides only indirect information about the tissue environment.[2] Using FA as an index for tract integrity oversimplifies a complex cellular environment, which is influenced by multiple factors. Diffusion metrics can vary in response to non-pathological changes in the tissue environment, such as neuronal packing density.[2] Non-aversive influences such as edematous tissue or crossing fibers may decrease anisotropy in a region without damaging tract integrity.[2] As such, analysis of diffusion tensor results should be done with a mind to the basis of the individual diffusion metrics and what aspect of the diffusion ellipsoid they represent.

Summary

DTI is a derivative of MRI that measures the diffusion of water molecules in tissue. DTI can be used to indirectly assess white matter integrity because the nature of diffusion changes based on the surrounding environment. FA, RD and AD are diffusion metrics which describe the degree of diffusion anisotropy, the diffusion perpendicular to the axon and the diffusion parallel to the axon, respectively. Changes in these metrics reflect pathological changes in white matter.

Diffusion tractography can also be used to create three-dimensional models of white matter tracts in-vivo. DTI provides a non-invasive measure of pathological changes in tissue which has promising application in stroke.

References

1. Butcher, K. & Emery, D. Acute stroke imaging. Part I: Fundamentals. *Can. J. Neurol. Sci.* **37,** 4–16 (2010).
2. Mori, S. & Zhang, J. Principles of diffusion tensor imaging and its applications to basic neuroscience research. *Neuron* **51,** 527–539 (2006).
3. Alexander, A. L., Lee, J. E., Lazar, M. & Field, A. S. Diffusion Tensor Imaging of the Brain. *Natl. Inst. Heal.* **4,** 316–329 (2008).
4. Neil, J. J. Diffusion imaging concepts for clinicians. *J. Magn. Reson. Imaging* **27,** 1–7 (2008).
5. Le Bihan, D. *et al.* Diffusion tensor imaging: concepts and applications. *J. Magn. Reson. Imaging* **13,** 534–46 (2001).
6. Beaulieu, C. The basis of anisotropic water diffusion in the nervous system - A technical review. *NMR Biomed.* **15,** 435–455 (2002).
7. Mori, S. & van Zijl, P. C. M. Fiber tracking: principles and strategies - a technical review. *NMR Biomed.* **15,** 468–80 (2002).
8. Qin, W. *et al.* Wallerian degeneration in central nervous system: Dynamic associations between diffusion indices and their underlying pathology. *PLoS One* **7,** 1–10 (2012).
9. Song, S.-K. *et al.* Dysmyelination Revealed through MRI as Increased Radial (but Unchanged Axial) Diffusion of Water. *Neuroimage* **17,** 1429–1436 (2002).
10. Budde, M. D. & Annese, J. Quantification of anisotropy and fiber orientation in human brain histological sections. *Front. Integr. Neurosci.* **7,** 3 (2013).
11. Cho, S. H. S.-H. *et al.* Motor outcome according to diffusion tensor tractography findings in the early stage of intracerebral hemorrhage. *Neurosci. Lett.* **421,** 142–6 (2007).

12. Yeo, S. S., Choi, B. Y., Chang, C. H. & Jang, S. H. Transpontine connection fibers between corticospinal tracts in hemiparetic patients with intracerebral hemorrhage. *Eur. Neurol.* **63,** 154–8 (2010).

13. Khalsa, S., Mayhew, S. D., Chechlacz, M., Bagary, M. & Bagshaw, A. P. The structural and functional connectivity of the posterior cingulate cortex: Comparison between deterministic and probabilistic tractography for the investigation of structure-function relationships. *Neuroimage* **102,** 118–127 (2014).

Chapter 3: Diffusion Tensor Imaging in ICH

Introduction

DTI has been used to investigate white matter changes in a wide variety of neurological disorders, such as apathy and depression,[1] white matter abnormalities in preterm infants,[2] and migraine.[3] Specific to stroke, DTI has been used to evaluate treatment of post-stroke aphasia[4] and ataxia, amongst others. In hemorrhage, DTI has been used primarily to evaluate Wallerian Degeneration and predict motor outcomes. These studies understandably focus on the CST, as will this review. A brief summary of the methodologies and findings from research in this area to date is presented below.

Wallerian Degeneration

Wallerian degeneration refers to a pattern of neural degeneration that occurs, usually within 2-3 days, after an injury that separates the axon from the soma.[5,6] First the axons distal to the site of injury start to disintegrate while the myelin sheath remains intact, followed by myelin degeneration and clearance of debris by the immune system.[5] A prominent difference between Wallerian degeneration in the central vs. peripheral nervous system is that total clearance of debris can take months to years in the former, compared to 1-2 weeks in the latter.[7]

Imaging Wallerian Degeneration

Wallerian degeneration can be visualized after injury as hypointense signal on T2-weighted MRI,[8] which correlates with functional outcome. Most hypointense signal changes occur chronically (>100 days after lesion), and T2 is less sensitive in the detection of Wallerian degeneration than DTI.[9] One study performed a direct comparison of T2-weighted imaging and DTI in the detection of Wallerian degeneration following chronic ischemic stroke. They found

that though T2-weighted images could detect differences between the ipsilateral and contralateral CST, DTI could discriminate diffusion changes in essentially all of their chronic stroke cases.[10] A similar comparison concluded that DTI was superior to T2 imaging in the detection of early-phase (within 2-weeks) Wallerian degeneration.[9] Using DTI, Wallerian degeneration changes are detectable as early as 2-3 days after lesion onset.[11]

Direct insight into the relationship between diffusion and pathology in Wallerian degeneration can be gained from combined DTI-histology studies. An excellent example is Qin et al.,[6] who measured diffusion indices at baseline and at 8 intervals between day 2-60 after CST transection in an animal model. FA, MD, AD and RD were measured in the pons, peduncle and internal capsule. Histological degeneration of the axons was observed at day 2, without any changes in myelin markers. This was accompanied by a significant day 2 decrease in FA and AD, and increase in RD, which continued gradually to day 8. During this time period, MD remained unchanged. In late-stage Wallerian degeneration (day 8-60) microglia activation and myelin clearance were observed.[6] This was accompanied by a minor increase in FA, thought to be secondary to axonal sprouting. MD and AD also increased slightly, potentially associated with myelin clearance, while RD remained unchanged.[6] Diffusion changes have also been observed in-vivo in humans after tract transection. Concha et al.[12] measured diffusion changes the corpus callosum of 3 epilepsy patients after surgical bisection. Consistent with previous studies, they found that AD was decreased at 1 week after the surgery, and RD was increased 2-4 months later.

Changes in Diffusion Over Time

The vast majority of studies in the current DTI-ICH literature measure FA at a single time-point, preventing comparison of FA changes over time. Two studies evaluated diffusion in the CST at

≥one time-point; both recorded FA out to day 90 and dichotomized results by patient outcome. FA in the CST in patients with poor motor outcome decreased gradually over time from baseline to day 90.[13,14] CST FA in patients with good motor scores either increased significantly[14] or remained stable over time.[13] The structural integrity of neurons decreases over time in Wallerian degeneration. Assessments in ischemic stroke suggest that anisotropy is decreased in regions with Wallerian degeneration.[10] Thus it makes intuitive sense that FA would decrease over time in degenerating tracts. Increases in FA in the CST during Wallerian degeneration have also been observed, and may be caused by axonal sprouting.[6]

Prediction of Motor Outcome in Stroke Using DTI

The vast majority of studies evaluating diffusion post-ICH indicate that FA in the CST is associated with motor outcome.[13,15–17] However, prediction appears to vary with the anatomical location where diffusion is measured.

The relationship between motor outcome and FA in the CST at the peduncle is particularly well established.[11,13,16] In the peduncle, relative FA (rFA) values (calculated as ipsilateral FA/contralateral FA) above 0.80 in the ipsilateral CST consistently predict good outcome,[11,18,19] and even FA above 0.45 can predict good outcome at 90 days.[13,14] One study measured FA at 2 weeks from onset in both the corona radiata and the CST. They found that despite observing more severe degeneration (median rFA value 0.732) in the corona radiata, rFA in the peduncles (median 0.848) was more predictive of motor score.[16] The authors speculated that MRI susceptibility effects from the adjacent hematoma may have confounded the FA data in the corona radiata, which was expected to be more clinically relevant. However, it seems more likely

that the peduncle is a better predictor of outcome because it is inferior to the stroke and thus experiences Wallerian degeneration.

Even hyper-acute measurements of FA can be sensitive predictors of outcome. FA in the peduncle measured within 24h of onset was related to 90-day motor function with a sensitivity of 88% and specificity of 92%.[14] A second study found that rFA in the peduncle measured ≤2 days of onset was predictive of 30-day outcome.[11]

MD, RD and AD Changes After ICH

In addition to FA, MD is commonly measured in studies of diffusion in the CST after ICH. However, it consistently fails to predict motor outcome.[20–22] Three studies found that MD was not significantly different between patients and controls.[11,21,23] Wang et al[18] reported a trend-level difference in MD between the ipsi- and contra-lateral sides of the peduncle at 3 days.[18]

To our knowledge, there are no clinical studies of diffusion in the CST in primary ICH that report AD or RD values. The lack of these measurements in clinical ICH DTI literature is surprising given their usefulness in understanding diffusion changes. DTI studies of Wallerian degeneration after ischemic stroke report AD and RD more commonly. In general, they find acutely reduced FA, increased AD, and decreased RD in the CST distal to the ischemic lesion.[9,10]

Relationship between Diffusion and Hematoma Volume

Only 3 studies in the ICH-CST literature included an assessment of ICH volume in their diffusion analysis. Koyama et al. found that acute hematoma volume in their 32-patient study was significantly correlated with rFA in the peduncle at 14-18 days.[17] On the other hand, Yoshioka et al.[20] found no relationship between acute hematoma volume and rFA measured in 17 patients within 5 days of onset. Finally, a study of 48 ICH patients found that patients with

severely decreased tract integrity (determined using a qualitative visual assessment of tractography results) had larger ICH volumes. However, this study was qualitative and did not report FA values, so the ability to assess a quantitative relationship was non-existent.[24]

It is notable that none of these studies used planimetric techniques to assess ICH volume, more commonly using estimation techniques which are known to overestimate lesion size.[25] In addition, none of the studies reported AD or RD values, which would provide useful information on the nature of pathological changes underlying diffusion.

Diffusion Metrics in Perihematoma Edema

Only one study of CST diffusion has accounted for the effects of perihematoma edema. FA was measured in 48 patients at 7±5 days, using a single small ROI placed in the region where the CST passed through the edema.[24] rFA in this region was 0.6±0.03 and rMD was 1.4±0.4, and neither were associated with motor outcome. The finding that FA in this region was decreased but was not related to motor outcome suggests that perihematoma edema is not associated with tract impairment. However, this study suffered from a number of issues: first, estimation of the region where the edema and CST overlapped was simplistic and inexact, and the small ROI would have been susceptible to partial volume effects. The study used only a single time point and lacked AD/RD measurements, making it difficult to determine details of microstructural changes in the region.

Conclusion

DTI can be used to assess Wallerian degeneration in the CST after ICH. FA and AD are commonly measured but only FA correlates with motor outcomes. Higher acute rFA ($\geq$0.80) is

indicative of good motor outcome. Over time, FA in patients with poor motor outcome decreases, while FA in patients with good motor scores does not. Pierpaoli et al[10] noted that diffusion anomalies could be observed in regions along the whole CST after stroke. However, it does not follow that all regions of the CST are equally predictive of outcome, and studies of FA along the CST reflect this. FA in the CST is especially predictive of motor outcome when measured at the level of the cerebral peduncle. Thus it is important to take into account the location of the measurement along the tract.

There remain a number of gaps in the literature. Diffusion studies evaluating motor outcome after ICH are primarily small, single-time point, ROI-based, measurements of FA. Only a minority of studies investigated a relationship between hematoma /edema and diffusion in the CST. RD and AD values in the CST have not been assessed in this literature and should be included in all future studies in this area.

References

1. Hollocks, M. J. *et al.* Differential relationships between apathy and depression with white matter microstructural changes and functional outcomes. *Brain* **138,** 3803–3815 (2015).
2. Benders, M. J. N. L., Kersbergen, K. J. & de Vries, L. S. Neuroimaging of White Matter Injury, Intraventricular and Cerebellar Hemorrhage. *Clinics in Perinatology* **41,** 69–82 (2014).
3. Neeb, L. *et al.* No microstructural white matter alterations in chronic and episodic migraineurs: A case-control diffusion tensor magnetic resonance imaging study. *Headache* **55,** 241–251 (2015).
4. Wan, C. Y., Zheng, X., Marchina, S., Norton, A. & Schlaug, G. Intensive therapy induces contralateral white matter changes in chronic stroke patients with Broca's aphasia. *Brain Lang.* **136,** 1–7 (2014).
5. Yamada, Kei; Patel, Uresh; Shrier, David; Tanaka, Hisashi; Chang, Ja-Kwei; Numaguchi, Y. MR Imaging of CNS tractopathy: Wallerian and Transneural Degeneration. *AJR* **171,** 813–18 (1998).
6. Qin, W. *et al.* Wallerian degeneration in central nervous system: Dynamic associations between diffusion indices and their underlying pathology. *PLoS One* **7,** 1–10 (2012).
7. Vargas, M. E. & Barres, B. A. Why Is Wallerian Degeneration in the CNS So Slow? *Annu. Rev. Neurosci.* **30,** 153–179 (2007).
8. Sawlani, V., Gupta, R. K., Singh, M. K. & Kohli, A. MRI demonstration of Wallerian degeneration in various intracranial lesions and its clinical implications. *J. Neurol. Sci.* **146,** 103–108 (1997).
9. Thomalla, G. *et al.* Diffusion tensor imaging detects early Wallerian degeneration of the

pyramidal tract after ischemic stroke. *Neuroimage* **22,** 1767–1774 (2004).

10. Pierpaoli, C. *et al.* Water diffusion changes in Wallerian degeneration and their dependence on white matter architecture. *Neuroimage* **13,** 1174–85 (2001).
11. Kusano, Y. *et al.* Prediction of functional outcome in acute cerebral hemorrhage using diffusion tensor imaging at 3T: a prospective study. *AJNR. Am. J. Neuroradiol.* **30,** 1561–5 (2009).
12. Concha, L., Gross, D. W., Wheatley, B. M. & Beaulieu, C. Diffusion tensor imaging of time-dependent axonal and myelin degradation after corpus callosotomy in epilepsy patients. *Neuroimage* **32,** 1090–1099 (2006).
13. Kuzu, Y. *et al.* Prediction of motor function outcome after intracerebral hemorrhage using fractional anisotropy calculated from diffusion tensor imaging. *Cerebrovasc. Dis.* **33,** 566–573 (2012).
14. Ma, C., Liu, A., Li, Z., Zhou, X. & Zhou, S. Longitudinal study of diffusion tensor imaging properties of affected cortical spinal tracts in acute and chronic hemorrhagic stroke. *J. Clin. Neurosci.* **21,** 1388–1392 (2014).
15. Koyama, T., Marumoto, K., Uchiyama, Y., Miyake, H. & Domen, K. Outcome assessment of hemiparesis due to intracerebral hemorrhage using diffusion tensor fractional anisotropy. *J. Stroke Cerebrovasc. Dis.* **24,** 881–889 (2015).
16. Koyama, T., Marumoto, K., Miyake, H., Ohmura, T. & Domen, K. Relationship between diffusion-tensor fractional anisotropy and long-term outcome in patients with hemiparesis after intracerebral hemorrhage. *NeuroRehabilitation* **32,** 87–94 (2013).
17. Koyama, T. *et al.* Diffusion tensor imaging for intracerebral hemorrhage outcome prediction: comparison using data from the corona radiata/internal capsule and the

cerebral peduncle. *J. Stroke Cerebrovasc. Dis.* **22,** 72–9 (2013).

18. Wang, D.-M., Li, J., Liu, J.-R. & Hu, H.-Y. Diffusion tensor imaging predicts long-term motor functional outcome in patients with acute supratentorial intracranial hemorrhage. *Cerebrovasc. Dis.* **34,** 199–205 (2012).
19. Koyama, T., Tsuji, M., Miyake, H., Ohmura, T. & Domen, K. Motor outcome for patients with acute intracerebral hemorrhage predicted using diffusion tensor imaging: An application of ordinal logistic modeling. *J. Stroke Cerebrovasc. Dis.* **21,** 704–711 (2012).
20. Yoshioka, H. *et al.* Diffusion Tensor Tractography Predicts Motor Functional Outcome In Patients With Spontaneous Intracerebral Hemorrhage. *Neurosurgery* **62,** 97–103 (2008).
21. Yokoyama, K. *et al.* Diffusion tensor imaging in chronic subdural hematoma: correlation between clinical signs and fractional anisotropy in the pyramidal tract. *AJNR. Am. J. Neuroradiol.* **29,** 1159–63 (2008).
22. Yeo, S. S. *et al.* Periventricular white matter injury by primary intraventricular hemorrhage: a diffusion tensor imaging study. *Eur. Neurol.* **66,** 235–41 (2011).
23. Yeo, S. S. *et al.* Evidence of corticospinal tract injury at midbrain in patients with subarachnoid hemorrhage. *Stroke.* **43,** 2239–41 (2012).
24. Cheng, C.-Y. *et al.* Motor outcome of deep intracerebral haemorrhage in diffusion tensor imaging: Comparison of data from different locations along the corticospinal tract. *Neurol. Res.* **37,** 774–781 (2015).
25. Kothari, R. U. *et al.* The ABCs of measuring intracerebral hemorrhage volumes. *Stroke.* **27,** 1304–1305 (1996).

Chapter 4: Corticospinal Tract Disruption in Acute Intracerebral Hemorrhage is Related to Hematoma Volume

Introduction

Intracerebral Hemorrhage (ICH) is the second most common type of stroke[1] and has a devastating 40-50% mortality rate.[2] Acute hematoma volume is a powerful predictor of 30-day mortality in ICH patients.[3] It has been hypothesized that motor deficits in ICH survivors are related to hemorrhagic disruption of white matter tracts important in motor function.[4] For example, involvement of the internal capsule and premotor cortex is related to poor upper limb recovery in ICH patients.[5]

Diffusion tensor imaging (DTI) is an MRI sequence that can quantitatively assess white matter integrity in vivo. Fractional anisotropy (FA) is a DTI parameter that reflects the degree of diffusion directionality in a voxel, in a range from completely isotropic (FA=0) to completely anisotropic (FA=1). FA can assess changes in tissue microstructure, as values decrease in conditions associated with demyelination and disrupted axonal integrity.[6] Additional diffusion metrics of interest include: Mean Diffusivity (MD), which quantifies the average diffusion displacement, Axial Diffusivity (AD), which describes diffusion parallel to the axon and is associated with axonal integrity, and Radial Diffusivity (RD), which describes diffusion perpendicular to the axon and is associated with myelin integrity.[6] Individual white matter tracts can also be isolated and examined in three dimensions using diffusion tensor tractography.

The relationship between motor outcome and FA in the CST is well established in ICH patients.[7–11] However, there are a number of issues with the current literature. Previous studies of diffusion after ICH fail to measure AD and RD in the CST, and thus lack information about

pathology. Secondly, despite the known impact of the hematoma on patient outcome, few studies have examined the relationship between CST integrity and hemorrhage volume. Only three previous studies have related FA to hematoma volume, with opposing results.[11–13]

The goal of this study is to address these gaps in the literature by assessing the predictive value of ICH volume for FA, MD, RD and AD in the CST. Our hypotheses are that: 1) larger hematoma volumes will predict lower FA and 2) lower FA values will be associated with worse motor scores.

Methods

Patients and Controls

DTI data was prospectively collected in acute ICH patients presenting to the Emergency Department at the University of Alberta Hospital. Data was also obtained from patients recruited into the ongoing Intracerebral Hemorrhage Acutely Decreasing Arterial Pressure Trial II (ICH ADAPT II; clinicaltrials.gov NCT00963976). These patients were randomized to two different systolic blood pressure targets (<180 mmHg vs. 140 mmHg) within 6 hours of onset and imaged with serial MRI, including DTI. The presence of ICH was confirmed on CT scan. Patients were excluded if they had ICH of non-spontaneous etiology or a previous CST lesion visible on MRI. The study protocol was approved by the local human ethics committee and informed consent was obtained. Motor disability was assessed using a composite of the upper and lower extremity National Institutes of Health Stroke Scale (NIHSS) subscale (0=normal, 8=hemiplegia). Chart review by experienced raters (L.G. and K.B.) was used to estimate missing motor NIHSS values.

A single DTI scan was also obtained in controls with stroke risk factors (older age, history of atrial fibrillation) but no previous stroke.

Image Acquisition

Patients were serially imaged with DTI on a 1.5T Siemens Sonata MRI scanner and 8-channel head coil at 72h, 7 days, and 30 days post-ICH. DTI data was acquired with a single shot echo-planar imaging sequence with: 50 slices at 2.2 mm thick for an isotropic resolution of 2.2mm, matrix 50x96x96, FOV=212 mm, TR = 7700 ms, TE = 94 ms. Diffusion weighting was achieved with 30 diffusion sensitizing gradient directions of b=1000 s/mm^2, and 5 b=0 s/mm^2 images. DTI scan time was 4:39 minutes.

Hematoma and Edema Volume Measurement

Hematoma volumes were measured on CT, using planimetric techniques, at baseline and 24 hours, using Analyze 12.0[14] (Figure 4.1). Edema volume was measured on CT at baseline and 24h, using a threshold of 5-23 Hounsfield Units. Hematoma and edema volumes were manually outlined in each patient on the Mean of *b*=0 s/mm^2 image, and three-dimensional models or 'masks' were made in Explore DTI[15] (Figure 4.1, B & C).

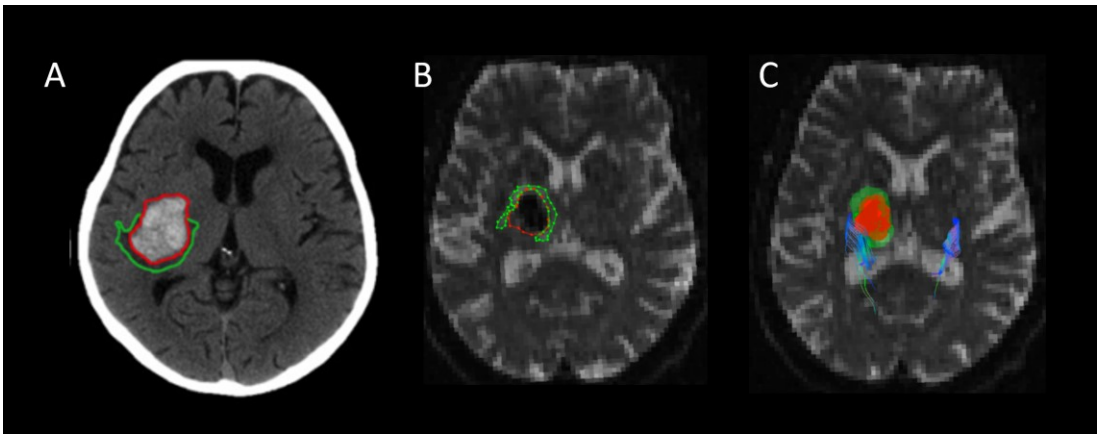

Figure 4.1 Measuring edema and hematoma. A) Regions of interest (ROIs) for hematoma (red) and edema (green) volumes are drawn planimetrically on the acute and 24h CT. B) ROIs are drawn on the 'Mean of b=0 s/mm^2' map. Green indicates edema, red the hemorrhage. C) The corticospinal tract is shown in blue in three-dimensions, adjacent to the hematoma and edema masks.

Diffusion Maps and Tractography

Diffusion images were post-processed as follows: 1) visual assessment of raw DICOMs and removal of directions with missing slices or movement, up to a maximum removal of 6 directions, 2) Conversion from DICOM to NIFTI format using MRICron,[16] 3) Eddy current /EPI distortion correction and derivation of FA, RD, RA and MD maps using Explore DTI.[15]

Diffusion tensor tractography was used to create three-dimensional models of the ipsilateral and contralateral CST in each patient (left and right CST in controls), using Explore DTI. Seed ROIs were placed on the colour FA maps in the mid pons and either the peduncle or corona radiata,

depending on lesion location (Figure 4.2). Deterministic tractography was performed using an FA threshold of 0.2 and 30° termination angle.

Diffusion values were averaged within the entire corticospinal tract. This method was chosen instead of the common ROI-based method in order to get the best estimate of whole-tract diffusion, and to reduce partial volume effects. All tract diffusion was calculated as a weighted average of the number of streamlines per voxel.

Patients whose ipsilateral CST failed to track were assigned an ipsilateral FA of 0 as a representation of severely decreased FA, as per Hirai et al.[17]

Comparison of Patient and Control CST

The mean of the FA, MD, AD and RD values in the left and right control CST were calculated to provide a single standard of healthy tracts for each diffusion measure. Control diffusion was compared with the ipsilateral patient CST to assess the diffusion changes associated with ICH.

In order to normalize diffusion metrics within patients, a measure of relative diffusion was calculated as:

(1) $$\text{Relative diffusion} = \frac{\text{Diffusion in ipsilateral CST}}{\text{Diffusion in contralateral CST}}$$

for each of relative FA (rFA), relative MD (rMD), relative AD (rAD) and relative RD (rRD).

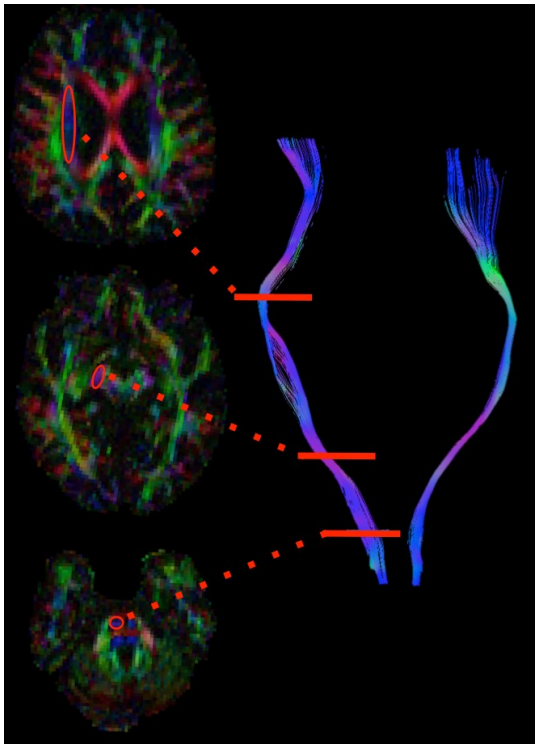

Figure 4.2 Reconstruction of the corticospinal tract (CST) in an example control subject. Left: seed locations shown on colour FA maps. Red indicates left-right tract orientation, green is for anterior-posterior orientation, and blue for superior-inferior orientation. Right: the resulting three-dimensional reconstruction of the CST. FA was measured along the entire length of each reconstructed tract.

Inter-scan Variation Analysis

An inter-scan variation analysis was performed in 4 healthy control subjects to assess the scan-rescan reliability of the longitudinal DTI data. Subjects were scanned three times over a 1-week period for a total of 12 scans. The MRI scanner, DTI scan protocol and diffusion tractography analysis of the CST was identical to that received by patients.

Inter-scan variation was assessed by comparing the variation in diffusion from the 12 control scans with the longitudinal diffusion changes observed in patients. First, the longitudinal change in CST relative diffusion (ΔrDiffusion) for each patient was calculated as:

(2) $$\Delta rDiffusion_{72h\text{-}Day\ 7} = rDiffusion_{Day7} - rDiffusion_{72h}$$

and

(3) $$\Delta rDiffusion_{Day\ 7\text{-}Day\ 30} = rDiffusion_{Day30} - rDiffusion_{Day7}$$

Second, the within-subject standard deviation (WSSD) for diffusion in the CST was calculated as:

(4) $$Mean\ WSSD = Mean\ (SD_{Subject\ 1\ over\ all\ scans},\ SD_{Subject\ 2\ over\ all\ scans},\ SD_{Subject\ 3\ over\ all\ scans},\ SD_{Subject\ 4\ over\ all\ scans})$$

This was calculated for each of FA, MD, AD and RD in the CST. The mean WSSD was then used as a threshold to determine the validity of each ΔrDiffusion in the longitudinal patient data. ΔrDiffusion >-1WSSD was considered a decrease, ΔrDiffusion >1WSSD was considered an increase. ΔrDiffusion ≤1WSSD was considered 'no change' and indicated that the changes in patient diffusion did not exceed scanner variability.

White Matter Hyperintensity Assessment

To assess the potentially confounding contribution of white matter disease to the relationship between CST integrity and ICH volume, white matter hyperintensity (WMH) load was measured on the first available FLAIR image of patients and controls. Severity of WMH was assessed using the modified Fazekas Scale,[18] where periventricular and deep WMH are rated together on a scale of 0 (absent), 1 (mild), 2 (moderate) and 3 (severe). Volume of WMH was measured planimetrically on the first available FLAIR using Quantimo.[19]

Statistical Analyses

Statistical analyses were performed with SPSS (v.22.0). FA values had primarily non-normal distribution while MD, AD and RD were normal, so statistical measures for each diffusion measure were chosen accordingly. Change in hematoma volume was assessed with a Wilcoxon Signed Rank Test. Fazekas score distribution between patients and controls was tested with a χ^2 analysis. Median WMH volumes were compared with the Mann-Whitney U test. A Kruskal-Wallis test with Dunn's post-hoc was used for comparisons of diffusion in the control and patient CST. Diffusion metrics were compared between the ipsilateral and contralateral patient CST using Paired T-tests or Wilcoxon Signed Rank Test.

Changes over time in relative diffusion were tested with both independent and repeated-measures tests. Cross-sectional analyses were performed with Kruskal-Wallis tests or a One-Way ANOVA as appropriate. Longitudinal comparisons of diffusion were conducted with Paired T-tests or Wilcoxon Signed Rank tests as appropriate. The relationships between diffusion values and ICH volume or motor outcome were assessed using linear regression and Kendall's Tau b correlation, respectively. Hematoma volumes were natural-log transformed to normalize distribution prior to being used in the regression analyses.

Results

Patient & Control Characteristics

Eighty-five patients with acute spontaneous ICH were recruited. Thirty-six patients were included in the study after exclusion for: lack of DTI (n=34); previous CST lesion (n=7); screen fail (n=4) and insufficient image quality (e.g. severe movement, n=4).

DTI scan times were acquired at the following time points: 72h (median time to imaging 40.8 [18.6] hours, n=22), Day 7 (7.6 [3.0] days, n=25), and Day 30 (31.7 [4.1] days, n=12). The number of scans received varied by patient: 18 (50%) patients received only a single scan, 8 (22%) patients were scanned at both 72h and day 7, 4 (11%) patients were scanned at day 7 and day 30, 1 (3%) patient had a scan at 72h and Day 30, and a total of 5 (14%) patients had scans at all 3 time points (Figure 4.3). Patients with three consecutive scans and two consecutive scans were grouped together for the longitudinal analyses.

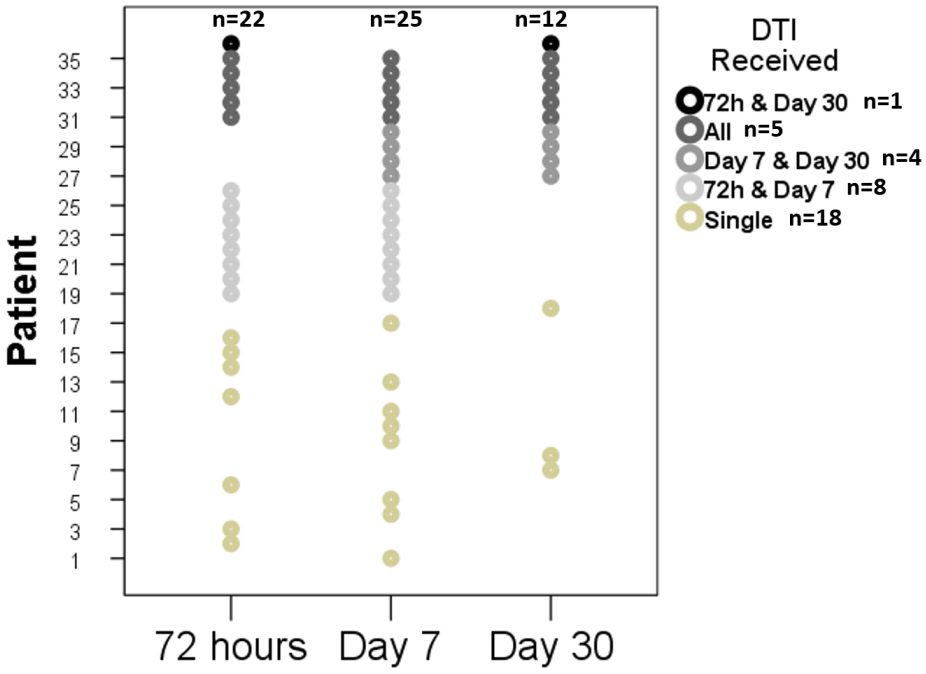

Figure 4.3 Distribution of patient imaging time-points. Patients with three consecutive scans and two consecutive scans were grouped together for the longitudinal analyses.

Median hematoma volume increased significantly from 8.9 (25.0) ml at the acute CT to 13.4 (40.5) ml at the 24h CT (p=0.038). Mean hematoma growth was 7.1±17.5 ml between baseline and 24h. Patient NIHSS and motor scores are listed in Table 4.1.

Table 4.1: Patient and Control Characteristics

PATIENTS, n=36	
Age (mean±SD), y	68±13
Men	19 (53%)
Medical History	
Hypertension	21 (58%)
Previous stroke	4 (11%)
NIHSS total score (Median, IQR)	
Admission, n=35	10 (14)
72 Hours, n=31	7 (15)
Day 7, n=25	5 (12)
Day 30, n=11	3 (10)
Day 90, n=28	2 (6)
NIHSS motor score	
Admission, n=35	3 (7)
72 Hours, n=33	3 (7)
Day 7, n=29	3 (7)
Day 30, n=14	5 (7)
Day 90, n=32	1 (4)
Lesion Location	
Basal Ganglia	13 (36%)
Lobar	12 (33%)
Thalamus	9 (25%)
Brainstem	2 (6%)
CONTROLS, n=11	
Age	62±13
Males	9 (82%)
NIHSS total score	0

DTI=Diffusion tensor imaging; IQR=inter-quartile range; y=year; SD=standard deviation; NIHSS=National Institute of Health Stroke Scale.

A total of eleven controls with stroke risk factors but no previous stroke were recruited. Patient and control subject ages (control mean age: 62±13 vs patient mean age: 68±13; p=0.162) and gender ratios (Control males = 9; Patient males = 19; p=0.086) were not significantly different.

Qualitative Tractography Findings

Qualitative changes in CST tractography were observed over time (Figure 4.4). Tractography failed to produce ipsilateral CST tracking results in 5 patients (Table 4.2). Imaging data analysis revealed no evidence of artifact, however, these patients had large hematomas overlapping the ipsilateral CST and impaired motor outcome at day 90. The tracking results were thus considered to be non-artifactual and the ipsilateral CST was assigned an FA of 0. The same could not be done for the other diffusion metrics, so the 5 patients with non-tracking ipsilateral CSTs were removed from the MD, AD and RD analyses. All contralateral CSTs were successfully reproduced by the tractography algorithm, regardless of hematoma volume.

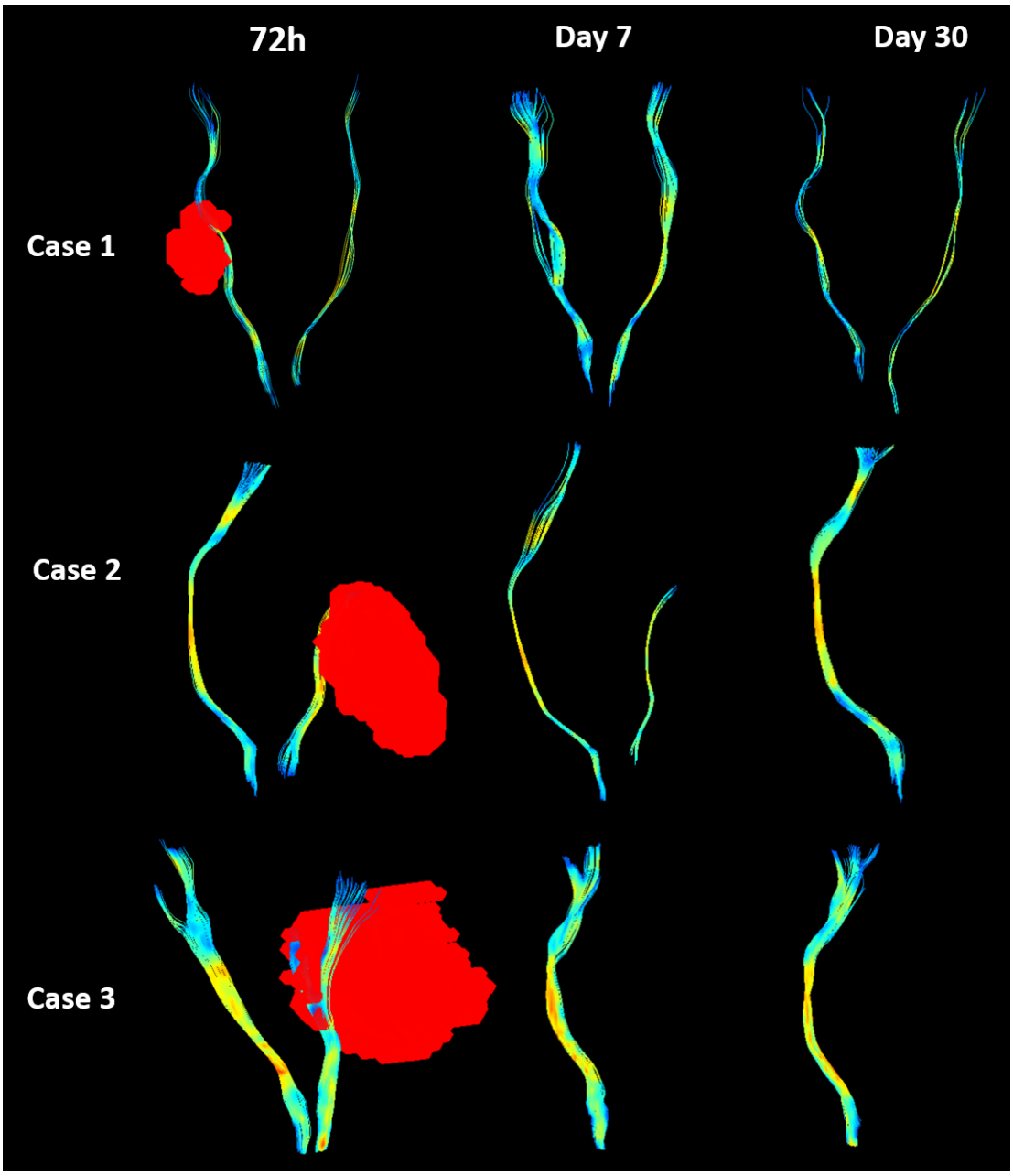

Figure 4.4 Example of qualitative tractography results in 3 patients with scans at 72h, Day 7 and Day 3. Note the lack of ipsilateral CST in Cases 2 & 3, which had large lesions that directly overlapped with the tract. Tracts are colour-coded by Fractional Anisotropy (FA), with warmer colours indicating increased FA.

Table 4.2: Characteristics of Patients with Non-Tracking Ipsilateral CSTs

Patient ID	Tracking @ 72h*	Tracking @ Day 7	Tracking @ Day 30	Volume, ml	Spatial Relationship	Day 30 Motor Score
38	✓	No Scan	×	29	CST displaced	8
40	×	No Scan	No Scan	37	CST displaced	7
48	✓	✓	×	41	CST displaced	7
52	✓	×	×	60	CST displaced	8
104	No Scan	✓	×	25	CST displaced	4

CST=corticospinal tract; ICH= Intracerebral Hemorrhage. CST displaced indicates that the ICH displaced the CST. *✓ indicates that the ipsilateral CST tracked successfully at that imaging time-point, × indicates failure to track, and 'No Scan' indicates that the patient did not receive DTI imaging.

Inter-scan Variation Analysis

Four healthy volunteers (mean age 24±1.2 years, three males) were scanned 3 times within 1 week for a total of 12 scans. The $\Delta rDiffusion_{72h\text{-}Day7}$ was calculated in 13 patients with consecutive scans at 72h and day 7, and $\Delta rDiffusion_{Day7\text{-}Day30}$ in 9 patients with scans at both day 7 and day 30. The mean WSSD and mean of ΔrDiffusion are listed in Tables 4.4 and 4.5.

White Matter Hyperintensities and Diffusion in the CST

Patient and control Modified Fazekas scores are outlined in Table 4.3. Distributions of modified Fazekas score was not different between patients and controls ($\chi^2(3) = 5.9$, p=0.115). Median WMH volume was also similar in patients (9.5 [26.3] ml) and controls (0.00 [15.0] ml; p=0.051).

Table 4.3: White Matter Hyperintensity Scores in Patients and Controls

Modified Fazekas Score	Patients (n=36)	Controls (n=11)
Absent	7 (19%)	6 (54%)
Mild	13 (36%)	3 (23%)
Moderate	11 (31%)	2 (18%)
Severe	5 (14%)	0 (0%)

Diffusion in the Control and Patient CST

Mean control FA (0.49±0.03) was significantly higher than the patient ipsilateral FA at each time point: 72h (0.42±0.10, p=0.016), Day 7 (FA 0.42±0.10, p=0.017) and Day 30 (0.29±0.22; p=0.001).

Patient ipsilateral MD was increased compared to the control MD (0.72±0.03 $x10^{-3}$ mm^2/s) at 72h (0.80±0.06 $x10^{-3}$ mm^2/s, p=0.001), and Day 7 (0.77±0.06 $x10^{-3}$ mm^2/s, p=0.047) but was not different at Day 30 (0.78±0.04 $x10^{-3}$ mm^2/s; p=0.073).

AD in the control (1.2±1.1 $x10^{-3}$ mm^2/s) and patient ipsilateral CST was similar at each time: 72h (1.2±0.08 $x10^{-3}$ mm^2/s), day 7 (1.2±0.10 $x10^{-3}$ mm^2/s), and day 30 (1.2±0.10 $x10^{-3}$ mm^2/s; p=0.204).

RD in the control CST (0.50±0.03 $x10^{-3}$ mm^2/s) was significantly lower than the ipsilateral patient CST at all times: 72h (0.59±0.05 $x10^{-3}$ mm^2/s, p<0.0001), Day 7 (0.57±0.05 $x10^{-3}$ mm^2/s, p=0.003), and Day 30 (0.58±0.03 $x10^{-3}$ mm^2/s; p=0.005).

Diffusion in the Ipsilateral and Contralateral Patient CST

Mean FA in the ipsilateral CST was lower than the contralateral tract at 72h (ipsi: 0.42±0.10 vs. contra: 0.48±0.04, n=22; p=0.028), and Day 7 (ipsi: 0.42±0.10 vs. contra: 0.49±0.03, n=25, p=0.018). However, there was no significant difference at Day 30 (ipsi: 0.29±0.22 vs. contra: 0.47±0.04, n=12**;** p=0.109).

MD in the ipsilateral CST was not significantly different compared to the contralateral tract at any time: 72h (ipsi: 0.80±0.06 $x10^{-3}$ mm^2/s vs. contra: 0.77±0.06 $x10^{-3}$ mm^2/s; p=0.065), Day 7 (ipsi: 0.77±0.06 $x10^{-3}$ mm^2/s vs. contra: 0.78±0.07 $x10^{-3}$ mm^2/s; p=0.471), or Day 30 (ipsi: 0.78±0.04 $x10^{-3}$ mm^2/s vs. contra: 0.78±0.08 $x10^{-3}$ mm^2/s; p=0.833).

AD in the ipsilateral CST was not different compared to the contralateral tract at 72h (ipsi: 1.22±0.08 $x10^{-3}$ mm^2/s vs. contra: 1.23±0.08 $x10^{-3}$ mm^2/s; p=0.451) or day 30 (ipsi: 1.18±0.10 $x10^{-3}$ mm^2/s vs. contra: 1.24±0.10 $x10^{-3}$ mm^2/s; p=0.020). However, at day 7 the ipsilateral CST was significantly decreased (1.18±0.10 $x10^{-3}$ mm^2/s) compared to the contralateral (1.25±0.10 $x10^{-3}$ mm^2/s).

Mean RD in the ipsilateral CST was increased compared to the contralateral tracts at 72h (ipsi: 0.59±0.05 $x10^{-3}$ mm^2/s vs. contra: 0.55±0.06 $x10^{-3}$ mm^2/s; p=0.004), but not at Day 7 (ipsi: 0.57±0.05 $x10^{-3}$ mm^2/s vs. contra: 0.55±0.06 $x10^{-3}$ mm^2/s; p=0.214), or Day 30 (ipsi: 0.58±0.27 $x10^{-3}$ mm^2/s vs. 0.56±0.08 $x10^{-3}$ mm^2/s; p=0.375)

Diffusion and Hematoma Volume

Acute hematoma volume did not predict rFA at 72h (β=-0.061, 95% Confidence Interval (CI): [-0.13-0.12]; p=0.097, n=22) or at day 7 (β = -0.19, [-0.11-0.04]; p=0.368; n=25). Larger acute

hematoma volumes predicted lower rFA at day 30 (β= -0.77 [-0.47- -0.13], p=0.003; n=12, Figure 4.5). Multivariate regression using WMH volume and rFA at day 30 as independent variables did not affect the relationship between hematoma volume and rFA (β=-0.19, [-0.03-0.13], p=0.383).

Hematoma volume was not related to rMD at 72h (β=0.158, [-0.15 -0.03], p=0.494) or Day 7 rMD (β =-0.115, [-0.04-0.03], p=0.591). Larger volumes predicted increased rMD at Day 30 (β=0.892, [0.03- 0.08], p=0.003, Figure 4.5). The addition of WMH volume to the regression did not affect the relationship between ICH volume and rMD at 30 days (β= -0.126, [-0.04-0.003], p=0.591).

rAD was not related to hematoma volume at 72h (β= -0.15, [-0.03-0.02], p=0.516), day 7 (β=-0.02, [-0.04-0.03], p=0.923) or day 30 (β= 0.47, [-0.03 - 0.09], p=0.245).

rRD was not predicted by acute hematoma volume at 72h (β=-0.10, [-0.11-0.07], p=0.645) or day 7 (β= -0.34, [-0.15-0.13], p=0.096). At day 30, larger ICH volume predicted an increase in rRD (β=-0.67, [-0.51- -0.06], p=0.018; Figure 4.5). This relationship was not affected by the addition of WMH volume (β=0.344, [-0.004-0.011], p=0.252).

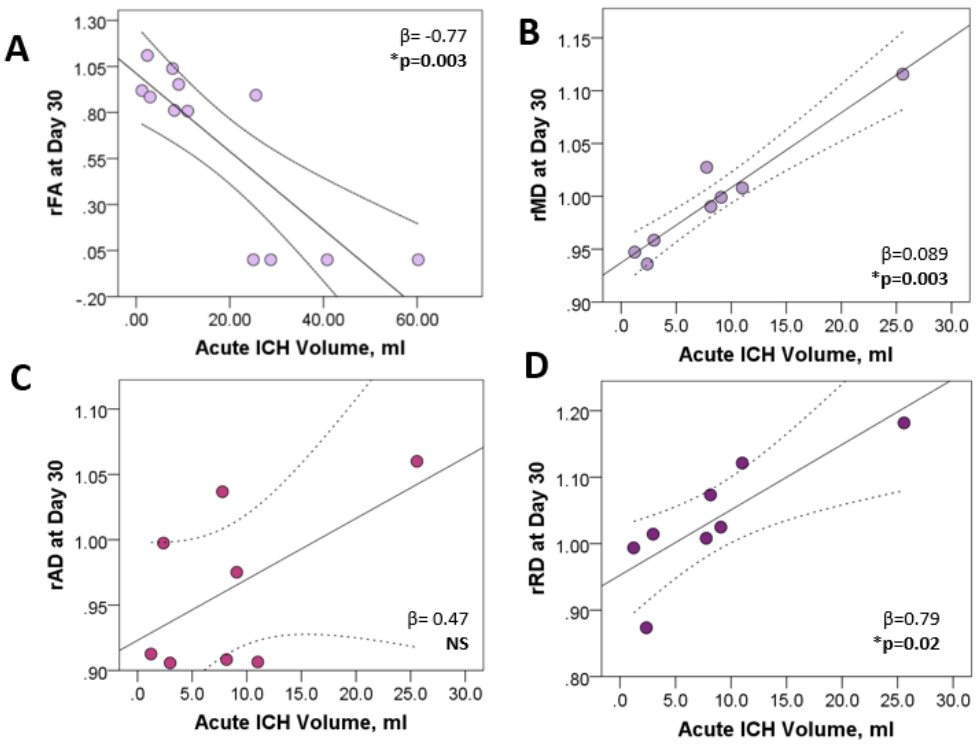

Figure 4.5 Linear regression analyses for diffusion and hematoma volume. Larger ICH volume predicted lower relative Fractional Anisotropy (rFA), increased relative Mean Diffusivity (rMD), and increased relative Radial Diffusion (rRD) at day 30. Dotted lines are 95% confidence intervals.

Changes in Relative Diffusion over Time

Due to the mixed cross-sectional and longitudinal nature of our dataset, diffusion changes over time were assessed in 3 different ways. Cross-sectional analyses included all patients, while longitudinal tests indicated change over time in a smaller subset of patients with >1 consecutive scan. Due to the small sample size of the longitudinal comparisons, the inter-scan variation analyses were used to provide information on the variability of change within patients.

Cross-sectional analyses of rFA in the CST over time indicated that there was no difference between 72h (0.88±0.22), Day 7 (0.88±2.1; p=1.00), or Day 30 (0.63±0.48; p=0.256**)**. The trend in FA for each patient is visualized in Figure 4.6.

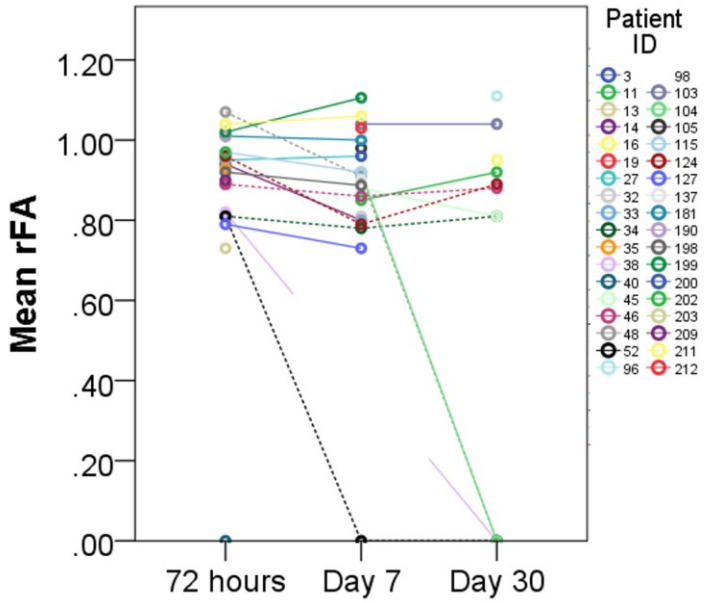

Figure 4.6 Plot of Relative Fractional Anisotropy (rFA) values at each time-point. Mean rFA in the CST is shown in 36 patients over time. Dotted lines indicate patients with diffusion data at all 3 time points (72h, day 7 and day 30).

The longitudinal analysis of rFA changes in patients with >1 consecutive scan showed a decrease in rFA between patients with scans at 72h (0.93±0.09) and day 7 (0.83±0.27; p=0.028, n=13) but not between patients with scans at day 7 and day 30 (0.59±0.45; p=0.889, n=9).

Consistent with the longitudinal findings, inter-scan variability indicated that rFA in the majority of patients (9 [69%]) decreased between 72h and day 7 (Figure 4.7). Between day 7 and day 30,

7 (78%) of patients experienced an increase in rFA compared to 2 (22%) experiencing a decrease (Table 4.5).

Cross-sectional analyses of rMD showed no change over time: 72h (1.0±0.06), day 7 (0.99±0.09), and day 30 (1.0±0.06; p=0.237). Longitudinal analyses were consistent with this finding: 72h-day 7 (1.1±0.07 vs day 7: 1.0±0.08, p=0.532, n=12) and day 7 - day 30 (1.0±0.06; p=0.312, n=6). Inter-scan variation data for rMD at 72h-day 7 was approximately split between increases (5 [43%]) and patients who had no change that surpassed scanner variability (4 [33%]) (Table 4.3). Between 7 and 30 days, 3 (50%) patients showed no real change in rMD, while 1 (17%) patient decreased and 2 (33%) increased (Table 4.5).

Cross-sectional analyses for rAD indicated that there was no difference over time in (72h: 0.99±0.06, day 7: 0.95±0.09 and day 30: 0.96±0.06; p=0.180). Longitudinal analyses also showed no change in rAD between 72h and day 7 (72h: 1.0±0.08 vs. day 7: 0.99±0.06; p=0.365, n=12) or between day 7 and day 30 (0.96±0.07, p=0.713, n=6). Inter-scan variation data for rAD at 72h-Day7 showed that 6 [50%] patients were increased. Between day 7-30 slightly more patients had increased (2 [33%]) than decreased (1 [17%]) but the majority (3 [50%]) experienced no change (Table 4.4 and 4.5).

rRD did not vary over time in the cross-sectional analysis (72h: 1.1±0.11, day 7: 1.0±0.11 and day 30: 1.0±0.09; p=0.406) or in the longitudinal analyses for changes between 72h and day 7 (72h: 1.1±0.10 vs. day 7: 1.1±0.12, n=12; p=0.0603) or between day 7 and day 30 (1.1±0.13; p=0.155, n=6). Inter-scan variation analyses indicated that between 72h and day 7 patients were evenly distributed between rRD increasing (4 [33%]) and decreasing (4[33%]). This was also true of day 7 and 30 (2 [33%] patients increased, 2 [33%] decreased).

Table 4.4: Inter-scan Variation Data for Relative Diffusion Changes from 72h to Day 7

Diffusion Measurement	Inter-scan Control Mean WSSD (10^{-3} mm^2/s)	Patient Mean of ΔrDiffusion$_{72h\text{-}Day7}$	Patients with decrease >1WSSD	Patients with increase >1WSSD	Patients with no change
FA (n=13)	0.0089	-0.0105	9 (69%)	3 (23%)	1 (8%)
MD (n=12)	0.0159	-0.0115	3 (25%)	5 (42%)	4 (33%)
AD (n=12)	0.0221	-0.0365	4 (33%)	6 (50%)	2 (17%)
RD (n=12)	0.0165	0.014	4 (33%)	4 (33%)	4 (33%)

WSSD indicates Within-subject Standard Deviation, a representation of test-retest scanner variability. Controls were 4 healthy subjects scanned 3 times over one week.

Table 4.5: Inter-scan Variation Data for Relative Diffusion Changes from Day 7 to Day 30

Diffusion Measurement	Inter-scan Control Mean WSSD (10^{-3} mm^2/s)	Patient Mean of ΔrDiffusion$_{Day7\text{-}Day30}$	Patients with decrease >1WSSD	Patients with increase >1WSSD	Patients with no change
FA (n=9)	0.0089	-0.1845	2 (22%)	7 (78%)	0
MD (n=6)	0.0159	-0.0264	1 (17%)	2 (33%)	3 (50%)
AD (n=6)	0.0221	-0.0094	1 (17%)	2 (33%)	3 (50%)
RD (n=6)	0.0165	-0.0489	2 (33%)	2 (33%)	2 (33%)

WSSD indicates Within-subject Standard Deviation, a representation of test-retest scanner variability. Controls were 4 healthy subjects scanned 3 times over one week.

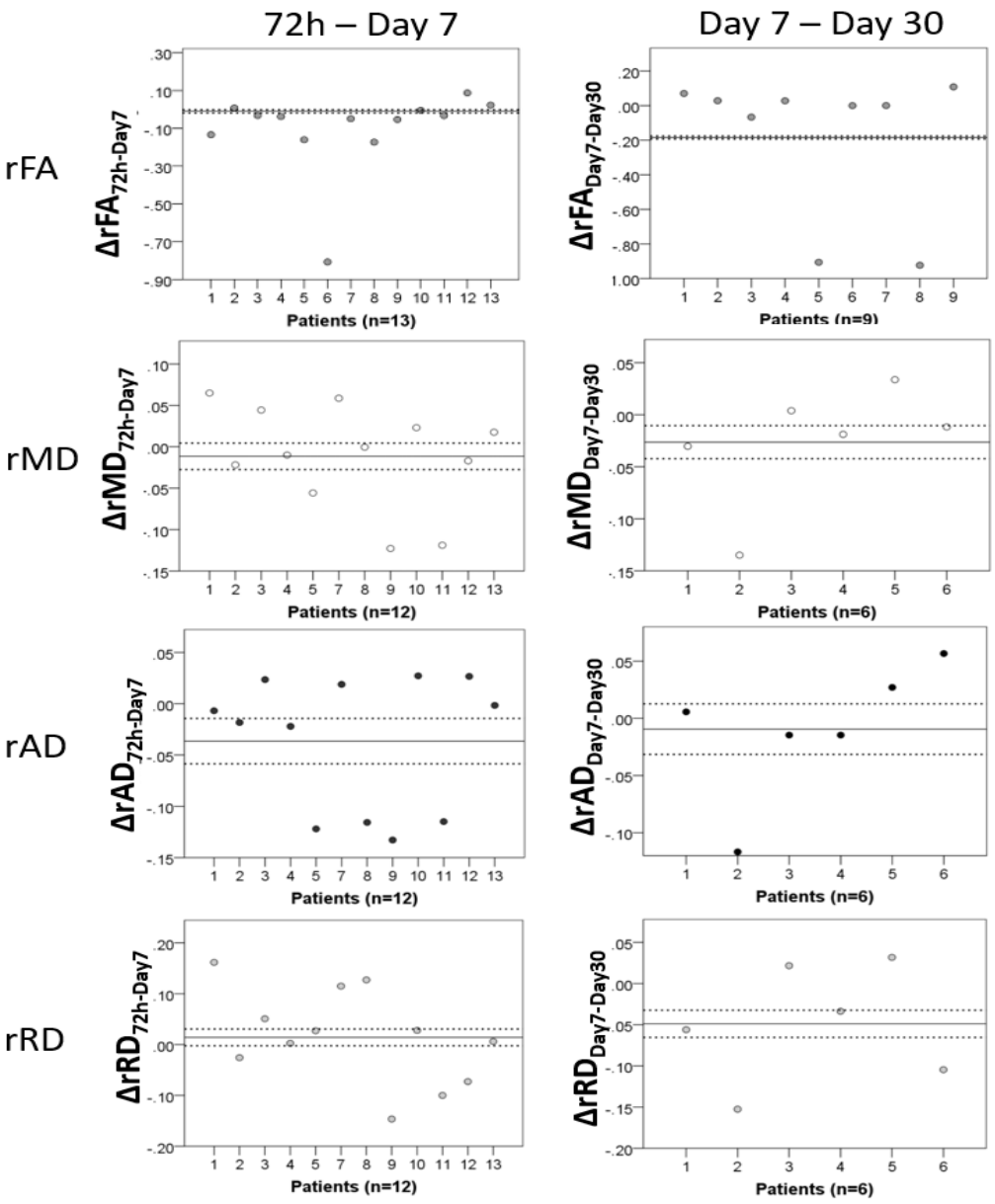

Figure 4.7 Change in relative diffusion over time with mean Within-Subject Standard Deviation (WSSD) thresholds. The centre line of each graph indicates the mean change in patient relative Diffusion (ΔrDiffusion) for each of rFA, rMD, rAD and rRD. Dotted lines indicate the +/-1 WSSD threshold used to determine the validity of each patient ΔrDiffusion. Note that the threshold and mean change lines are essentially merged for rFA

Diffusion and Motor Function

Worse motor function at day 90 was correlated with lower rFA at day 7 (τ_b=0.0439, p=0.008; Figure 4.8) but there was no relationship with rFA at 72h (τ_b =-0.224, p=0.202) or day 30 (τ_b= -0.364, p=0.143).

rMD was not correlated with day 90 motor scores at any time: 72h (τ_b= -0.082, p=0.652) day 7 (τ_b=0.245, p=0.154) or day 30 (τ_b=0.514, p=0.117), and neither was rAD (72h: τ_b=-0.247, p=0.176; day 7: τ_b= -0.089, p=0.604; day 30: τ_b=0.00, p=1.00).

rRD was not related to motor score at 72h (τ_b =-0.082, p=0.652). However, worse motor outcome was associated with increased rRD at day 7 (τ_b=0.367, p=0.033) and day 30 (τ_b=0.926, p=0.005).

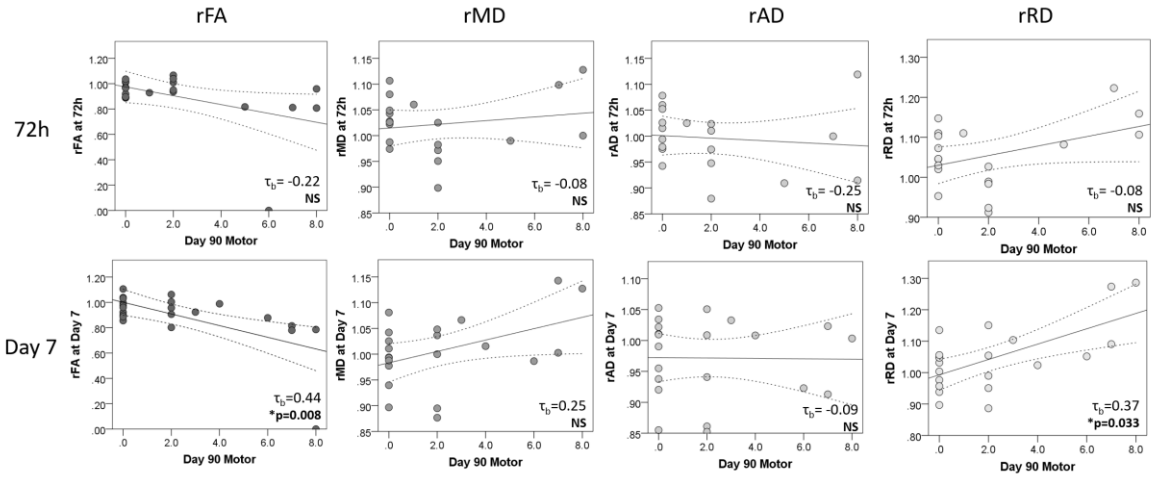

Figure 4.8 Correlation Analyses for Diffusion and Motor Score. National Institute of Health Stroke Scores at day 90 were correlated with relative Fractional Anisotropy (rFA), relative Mean Diffusivity (rMD), relative Axial Diffusion (rAD) and relative Radial Diffusion (rRD). Dotted lines indicate 95% confidence intervals. Increasing values of the motor scores indicates worse functional outcome.

Discussion

This study examines the potentially mediating effect of hematoma volume on tract integrity and motor outcome after ICH. We found that acute ICH volume predicted rFA, rMD, and rRD values at Day 30. Correlations with motor outcome were mixed, possibly due to the method of diffusion measurement utilized. Compared to controls, the ipsilateral patient CST showed decreased diffusion anisotropy and greater radial diffusion, which are associated with decreased tract and myelin integrity, respectively.

Qualitative Results

The three-dimensional nature of the tractography analysis allowed us to observe changes in the integrity of a single tract over time (Figure 4.4). In 5 patients with large hematoma volumes, the ipsilateral CST was reconstructed at the initial scan but failed to be reproduced at following time-points (Table 4.2). These qualitative tractography results suggest that tract integrity is maintained in the initial stages after the stroke, and decreases over time with Wallerian degeneration.

Diffusion in the CST

rFA in the ipsilateral CST was significantly decreased compared to controls and the contralateral tract. FA decreases represent a loss of diffusion orientation in the microstructure. Decreased FA after ICH is well-documented[7,8,20] and reflects decreased tract integrity and Wallerian degeneration.[21]

MD was not different between the patient ipsilateral and contralateral CSTs. This is consistent with previous studies which show that MD is stable during Wallerian degeneration, aside from a

slight chronic increase associated with myelin clearance.[22] MD is a measure of the amplitude of diffusion in a voxel and does not reflect directional changes such as FA, RD and AD.

AD was essentially unchanged in the ipsilateral CST compared to controls and the contralateral CST. AD represents diffusion parallel to the axon and previous studies have found that it decreases in the context of axonal injury.[22–24] AD typically decreases acutely in Wallerian degeneration.[22] Thus the lack of AD change in the ipsilateral CST may reflect a relative lack of axonal damage. However, it may also reflect the inability of our method to detect changes in diffusion, as will be discussed below.

RD in the ipsilateral CST was not significantly different compared to the contralateral. This indicates that the contralateral tract may also experience microstructural changes, though not to the extent that it affects FA measurements. RD was significantly increased in the contralateral tract compared to controls. RD reflects diffusion perpendicular to the tract, and increases have been associated with decreased tract integrity, particularly dysmyelination.[22,23] Thus our findings may reflect that integrity of myelin in the ipsilateral CST is reduced.

Diffusion Changes over Time

Group analyses showed little to no change over time in rFA, rMD, rRD and rAD. The inter-scan results indicated some variability within individual patient changes. These changes will be discussed below; however, they are viewed with the understanding that the sample size is very small (6-13 patients).

All versions of our analysis (longitudinal and inter-scan) indicated a decrease in rFA between 72h and day 7. This is consistent with studies that have shown FA decreases within the initial 1-

week period after ICH.[7,20,25] Between day 7 and 30 we found no statistical difference in rFA values, but inter-scan variation showed several patients increasing during this time (Figure 4.7). This may indicate that patients who were eligible to receive scans at day 30 had better tract integrity than patients who were scanned at 72h. Additionally, increases in FA in tracts experiencing Wallerian degeneration have been reported after day 8 and may represent axonal sprouting.[22]

Patients were approximately evenly distributed across the inter-scan change categories for rMD, rAD, and rRD, which is likely why results were non-significant at the group level. Slightly more patients (6 vs. 4) had an AD increase vs. a decrease between 72h and day 7 (Figure 4.7). The mix of 'increases' and 'decreases' in diffusion exhibited by patients may represent differences in their tract integrities, as some patients are likely to experience less CST degeneration than others. Previous studies of FA over time have dichotomized their results by patient outcome ('good' vs. 'poor'). They find that FA tends to decrease in patients with poor motor outcome, while FA increases or remains stable in patients with good outcome.[9,10] Our analysis was small and not grouped by outcome, but differences in outcome may explain the variation observed in the inter-scan analyses (Figure 4.7).

Few previous diffusion studies of the CST in ICH have measured FA at more than one time-point.[21,26] Though our ability to measure diffusion over time was significantly diminished by a small sample size and inconsistent longitudinal data, we remain the only study to provide information on changes in AD and RD in the CST over time after ICH.

Hemorrhage Volume and FA

In our study, larger hematoma volumes predicted decreased rFA, increased rMD, and increased rRD, but only at the latest time-point, day 30. There was no relationship between hematoma volume and diffusion at 72h or day 7. The differences between time points is likely to be a reflection of our method of diffusion measurement. We chose to average diffusion through the entire CST in a purposeful attempt to measure whole-tract change, rather than using a slice-based ROI method. However, this may have had the unintended result of averaging across injury-related diffusion changes. At initial time-points, Wallerian degeneration is less extensive and tract damage may not be significant enough to be reflected in our averaged FA. By day 30 however, Wallerian degeneration has progressed and the integrity of the entire tract is likely decreased, which is reflected as a significant FA change.

Previous studies have reported a relationship between hematoma volume and the CST.[13,25,27] Two of these failed to find an association between integrity and ICH volume. The first assessed the health of the CST using a qualitative categorization of tractography results (e.g. 'good' for tracts that appeared to be preserved around the hematoma vs. 'bad' for non-tracking CSTs). They found that hematoma volume (mean 18.1±14.3 ml) was significantly smaller in patients with more preserved CSTs.[13] However, this study was qualitative and did not report FA values, so they were not able to assess a quantitative relationship. The second study found no relationship between acute hematoma volume (13±9.6 ml) and rFA measured within 5 days of onset. rFA was measured in the section of the CST closest to the hematoma,[25] but did not incorporate the peduncle, which is most predictive of outcome.[7,21,27] Finally, a single study found that acute hematoma volume (range: 2.5-52.9 ml) was significantly correlated with rFA at 14-18 days.[27] Here, the CST was separated into the corona radiata and cerebral peduncle, and only the

peduncle showed a significant association with ICH volume. Thus inclusion of the peduncle appears to be important when using FA to interpret the effects of the hematoma. This is likely because the peduncle is distal to the hematoma and experiences Wallerian degeneration after injury.

FA & Motor Outcomes

We found that decreased rFA at day 7 was associated with worse motor function at 90 days post-ICH. This is consistent with previous studies that show a relationship between FA and motor outcome after ICH.[7,8,20] The lack of relationship between MD and motor score is consistent with previous studies.[12,13,28] MD does not represent microstructural change to the same extent as the other measures, and does not vary in the acute stages of Wallerian degeneration[22,29]

No previous studies have reported AD and RD with respect to motor outcome after ICH. We found that increased rRD at day 7 and day 30 was correlated with worse motor outcome, but that rAD was not related to motor outcome. The lack of relationship between motor score and AD, and for rFA at 72h and day 30, may be due to a number of factors. First, many previous studies correlate FA values with patient outcomes grouped by good/poor,[7,8,21] which improves the chance of finding a statistical relationship. Second, diffusion values were averaged along the entire CST, which appears to have the same effect on motor prediction as it did in correlations with hematoma volume. Previous studies with successful motor prediction tend to measure FA specifically in regions of Wallerian degeneration distal to the hematoma. They also often use single-slice ROIs, which provide a more precise assessment of tract injury[7,13,20] Comparatively, our whole-tract diffusion measurement is not ideal for predicting motor outcomes.

Limitations

The primary limitations of this study are the small sample size (n=36), and the mixed cross-sectional/longitudinal data. Longitudinal data collection was desirable, but was prohibited by the high morbidity and mortality in our patient population.

In addition, we chose to average the diffusion data throughout the CST with the goal of gaining a better measure of whole-tract integrity related to ICH volume. Measuring a larger region of the CST also reduces partial volume effects. However, prediction of motor outcome has been shown to be dependent on the location of diffusion measurement along the CST.[11,30] Because our method of measurement averages across regions of the tract that are differentially affected by the hematoma, we appear to have reduced both our ability to measure acute diffusion changes in the CST, and to predict motor outcomes.

Conclusion

This clinical study provides insights into the mechanisms of functional disability following hemorrhagic stroke. We found that DTI demonstrates evidence of CST disruption following acute ICH. Increased hematoma volume predicted decreased tract integrity in patient CSTs at day 30. Our method of averaging diffusion along the entire CST may be responsible for the inconsistent correlation between diffusion and motor outcomes. Overall, these findings suggest that hematoma volume is a mediating factor in white matter changes after ICH. Serial assessment with DTI in ICH is required to further define the relationship between larger hematoma volume, diffusion and functional outcome.

References

1. Grysiewicz, R. A., Thomas, K. & Pandey, D. K. Epidemiology of ischemic and hemorrhagic stroke: incidence, prevalence, mortality, and risk factors. *Neurol. Clin.* **26,** 871–95, vii (2008).

2. Gebel, J. M. & Broderick, J. P. Intracerebral hemorrhage. *Neurol. Clin.* **18,** 419–38 (2000).

3. Broderick, J. P., Brott, T. G., Duldner, J. E., Tomsick, T. & Huster, G. Volume of intracerebral hemorrhage. A powerful and easy-to-use predictor of 30-day mortality. *Stroke.* **24,** 987–993 (1993).

4. Cho, S. H. S.-H. *et al.* Motor outcome according to diffusion tensor tractography findings in the early stage of intracerebral hemorrhage. *Neurosci. Lett.* **421,** 142–6 (2007).

5. Lee, K. B. *et al.* The motor recovery related with brain lesion in patients with intracranial hemorrhage. *Behav. Neurol.* **1,** 1-6 (2015).

6. Mori, S. & Zhang, J. Principles of Diffusion Tensor Imaging and Its Applications to Basic Neuroscience Research. *Neuron* **51,** 527–539 (2006).

7. Kusano, Y. *et al.* Prediction of functional outcome in acute cerebral hemorrhage using diffusion tensor imaging at 3T: a prospective study. *AJNR. Am. J. Neuroradiol.* **30,** 1561–5 (2009).

8. Wang, D.-M., Li, J., Liu, J.-R. & Hu, H.-Y. Diffusion tensor imaging predicts long-term motor functional outcome in patients with acute supratentorial intracranial hemorrhage.

Cerebrovasc. Dis. **34,** 199–205 (2012).

9. Kuzu, Y. *et al.* Prediction of motor function outcome after intracerebral hemorrhage using fractional anisotropy calculated from diffusion tensor imaging. *Cerebrovasc. Dis.* **33,** 566–573 (2012).

10. Ma, C., Liu, A., Li, Z., Zhou, X. & Zhou, S. Longitudinal study of diffusion tensor imaging properties of affected cortical spinal tracts in acute and chronic hemorrhagic stroke. *J. Clin. Neurosci.* **21,** 1–5 (2014).

11. Koyama, T. *et al.* Diffusion tensor imaging for intracerebral hemorrhage outcome prediction: comparison using data from the corona radiata/internal capsule and the cerebral peduncle. *J. Stroke Cerebrovasc. Dis.* **22,** 72–9 (2013).

12. Yoshioka, H. *et al.* Diffusion Tensor Tractography Predicts Motor Functional Outcome In Patients With Spontaneous Intracerebral Hemorrhage. *Neurosurgery* **62,** 97–103 (2008).

13. Cheng, C.-Y. *et al.* Motor outcome of deep intracerebral haemorrhage in diffusion tensor imaging: Comparison of data from different locations along the corticospinal tract. *Neurol. Res.* **37,** 774–781 (2015).

14. Robb, R. A. *et al.* ANALYZE: A comprehensive, operator-interactive software package for multidimensional medical image display and analysis. *Comput. Med. Imaging Graph.* **13,** 433–454 (1989).

15. Leemans, A., Jeurissen, B., Sijbers, J. & Jones, D. ExploreDTI: a graphical toolbox for processing, analyzing, and visualizing diffusion MR data. in *Proceedings 17th Scientific Meeting, International Society for Magnetic Resonance in Medicine* **17,** 3537 (2009).

16. Rorden, C., Karnath, H.-O. & Bonilha, L. Improving lesion-symptom mapping. *J. Cogn. Neurosci.* **19,** 1081–1088 (2007).

17. Hirai, K. K., Groisser, B. N., Copen, W. A., Singhal, A. B. & Schaechter, J. D. Comparing prognostic strength of acute corticospinal tract injury measured by a new diffusion tensor imaging based template approach versus common approaches. *J. Neurosci. Methods* **257,** 204–213 (2016).

18. Pantoni, L. *et al.* Impact of age-related cerebral white matter changes on the transition to disability - The LADIS study: Rationale, design and methodology. *Neuroepidemiology* **24,** 51–62 (2005).

19. Kosior, J. C. *et al.* Quantomo: validation of a computer-assisted methodology for the volumetric analysis of intracerebral haemorrhage. *Int. J. Stroke* **6,** 302–305 (2011).

20. Yokoyama, K. *et al.* Diffusion tensor imaging in chronic subdural hematoma: correlation between clinical signs and fractional anisotropy in the pyramidal tract. *AJNR. Am. J. Neuroradiol.* **29,** 1159–63 (2008).

21. Kuzu, Y. *et al.* Prediction of motor function outcome after intracerebral hemorrhage using fractional anisotropy calculated from diffusion tensor imaging. *Cerebrovasc. Dis.* **33,** 566–573 (2012).

22. Qin, W. *et al.* Wallerian degeneration in central nervous system: Dynamic associations between diffusion indices and their underlying pathology. *PLoS One* **7,** 1–10 (2012).

23. Song, S. *et al.* Dysmyelination Revealed through MRI as Increased Radial (but Unchanged Axial) Diffusion of Water. *NeuroImage* **1436,** 1429–1436 (2002).

24. Beaulieu, C. & Allen, P. S. Determinants of anisotropic water diffusion in nerves. *Magn. Reson. Med.* **31,** 394–400 (1994).

25. Yoshioka, H. *et al.* Diffusion tensor tractography predicts motor functional outcome in patients with spontaneous intracerebral hemorrhage. *Neurosurgery* **62,** 97–103 (2008).

26. Ma, C., Liu, A., Li, Z., Zhou, X. & Zhou, S. Longitudinal study of diffusion tensor imaging properties of affected cortical spinal tracts in acute and chronic hemorrhagic stroke. *J. Clin. Neurosci.* **21,** 1388–1392 (2014).

27. Koyama, T., Marumoto, K., Miyake, H., Ohmura, T. & Domen, K. Relationship between diffusion-tensor fractional anisotropy and long-term outcome in patients with hemiparesis after intracerebral hemorrhage. *NeuroRehabilitation* **32,** 87–94 (2013).

28. Yeo, S. S. *et al.* Periventricular white matter injury by primary intraventricular hemorrhage: a diffusion tensor imaging study. *Eur. Neurol.* **66,** 235–41 (2011).

29. Thomalla, G. *et al.* Diffusion tensor imaging detects early Wallerian degeneration of the pyramidal tract after ischemic stroke. *Neuroimage* **22,** 1767–1774 (2004).

30. Tao, W.-D., Wang, J., Schlaug, G., Liu, M. & Selim, M. H. A Comparative Study of Fractional Anisotropy Measures and ICH Score in Predicting Functional Outcomes After Intracerebral Hemorrhage. *Neurocrit. Care* **21,** 417–25 (2014).

Chapter 5: Corticospinal Tract Integrity is Acutely Maintained Within Perihematoma Edema

Introduction

Intracerebral hemorrhage (ICH) represents 10-15% of stroke cases,[1] and is associated with significant disability.[2] Up to 80% of ICH survivors are unable to live independently 6 months after stroke.[3] Blood products, inflammatory cascades, and mass effect associated with the hematoma are detrimental to local parenchyma.[4–6] However, the etiology of perihematoma edema and its effect on white matter integrity is uncertain. Perihematoma edema has been commonly attributed to plasma extrusion during clot contraction.[7–9] Minor reductions in perihematoma blood flow have also been observed, suggesting the potential for secondary ischemia and injury of local white matter, such as the Corticospinal Tract (CST).[10–13] The absolute reductions in blood flow do not appear to be significant enough to result in ischemic injury in most cases, however.[14]

Diffusion Tensor Imaging (DTI) is an MRI sequence that can be used to indirectly assess CST integrity. Fractional Anisotropy (FA) is a measure of diffusion directionality, measured in a range from isotropic (FA=0) to anisotropic (FA=1), and reflects surrounding tissue microstructure. Additional diffusion metrics of interest include: Mean Diffusivity (MD), which quantifies the average diffusion displacement, Axial Diffusivity (AD), which describes diffusion displacement parallel to the axon, and Radial Diffusivity (RD), which is diffusion displacement perpendicular to the axon.[15]

We aimed to measure the integrity of the edematous CST over time, using planimetric edema measurement and multiple indices of diffusion. We hypothesized that the edematous CST would 1) have low FA relative to the contralateral tract and 2) predict motor score in ICH patients.

Methods

Patients

DTI data was prospectively collected in acute ICH patients presenting to the Emergency Department at the University of Alberta Hospital. Data was also obtained from patients recruited into the ongoing Intracerebral Hemorrhage Acutely Decreasing Arterial Pressure Trial II (ICH ADAPT II; clinicaltrials.gov NCT00963976). These patients were randomized to two different systolic blood pressure targets (<180 mmHg vs. 140 mmHg) within 6 hours of onset and imaged with serial MRI, including DTI. The presence of ICH was confirmed on CT scan. Exclusion criteria were: secondary ICH (non-spontaneous etiology), ICH location that did not allow edema to overlap with the CST, or a previous CST lesion visible on MRI. The study protocol was approved by the local human ethics committee and informed consent was obtained. Motor disability was assessed using a composite of the upper and lower extremity National Institutes of Health Stroke Scale (NIHSS) subscale (0=normal, 8=hemiplegia). Chart review by experienced raters (L.G. and K.B.) was used to estimate missing motor NIHSS values.

Image Acquisition

Patients underwent baseline diagnostic and follow-up CT scans 24 hours later. MRI including DTI was obtained at 48 hours, 7 days, and 30 days after ICH onset. DTI data was acquired on a 1.5T Siemens Sonata with an 8-channel coil and a single shot echo-planar imaging sequence with the following parameters: 2.2 mm isotropic resolution, 50 slices, matrix = 50x96x96 cm, FOV = 212mm, TR = 7700 ms, TE = 94 ms; total scan time = 4.6 minutes. Diffusion weighting was obtained with 30 diffusion gradient directions of b=1000 s/mm^2, and five b=0 s/mm^2 images.

Diffusion Image Analysis

Diffusion images were post-processed as follows: 1) visual assessment of raw DICOMs and removal of directions with missing slices or movement, up to a maximum removal of 6 directions, 2) Conversion from DICOM to NIFTI format using MRICron,[16] 3) Eddy current/EPI distortion correction and derivation of FA, RD, RA and MD maps using Explore DTI.[17] In order to model the CST, seeds were placed on the colour FA map in the mid-pons, and either the peduncle or corona radiata, depending on lesion location. Deterministic tractography was performed using an FA threshold of 0.2 and 30^{o} termination angle. All tract diffusion was calculated as a weighted average of the number of streamlines per voxel.

Regions of interest (ROIs) in the perihematoma edema and a region of contralateral healthy tissue were drawn on the 'mean of b=0 s/mm2' image (Figure 5.1A). To isolate the edematous CST, the three-dimensional tract was overlapped with the mask of the perihematoma edema (Figure 5.1B). The portion of the contralateral CST parallel to the edema was used as a healthy control (Figure 5.1C). FA, MD, RA and RD were measured in the perihematoma and contralateral edema, edematous CST, and contralateral CST. Relative diffusion measures were calculated as:

$$\text{(1)} \qquad \text{Relative diffusion} = \frac{\text{Diffusion in ipsilateral CST}}{\text{Diffusion in contralateral CST}}$$

for each of relative FA (rFA), relative MD (rMD), relative AD (rAD) and relative RD (rRD).

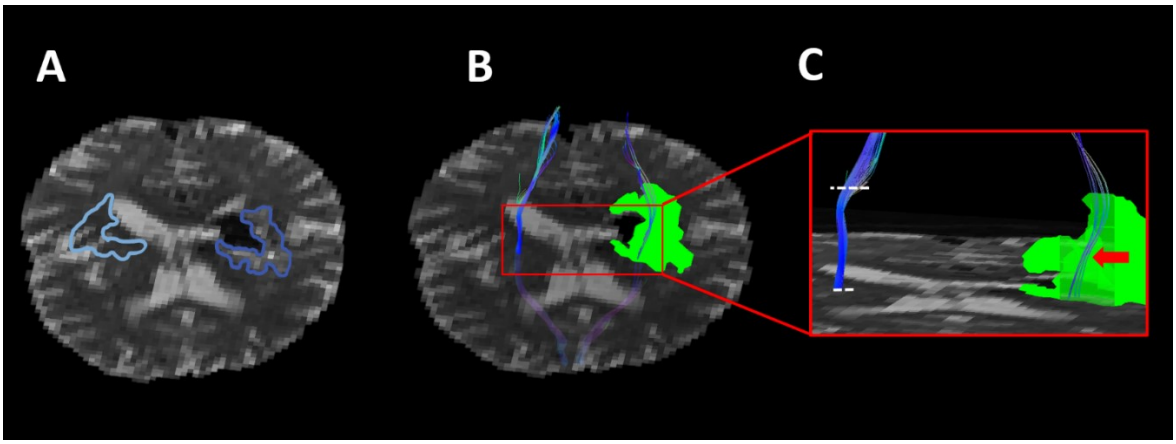

Figure 5.1. Measurement of Fractional Anisotropy (FA) in the edema and Corticospinal Tract (CST). Regions of interest are shown on the T2-weighted 'Mean of b=0 s/mm2' map. A) FA was measured in the perihematoma edema (dark blue) and contralateral area (light blue). B) The three-dimensional CST was overlapped with the mask of the edema (green). C) FA was measured in the portion of the CST passing through the edema (arrow), and in the portion of contralateral CST parallel to the edematous CST (dotted line).

Analysis of Tract Depth Within Edema

Manually outlining the perihematoma edema ROI on the non-diffusion-weighted (b=0 s/mm^2) image is associated with subjective variability in defining hematoma vs. edematous tissue. Voxels at the border of the edema are at highest risk of erroneous FA measurement resulting from misclassification and partial volume effects (PVE). To address this issue, FA in the edematous CST was categorized by voxel depth, ranging from "border voxels" at the border of the edema mask (1 voxel deep) to "deep voxels" within the center of the edema mask (≥3 voxels deep). Deep voxels were assumed to have less potential for misclassification and PVE, and tract FA in the border voxels was expected to be similar to FA in deep voxels.

Hematoma & Edema Volume Measurement

Hematoma volume was measured on CT scans using planimetric techniques. Edema volumes were measured on CT using planimetric techniques and a threshold of 5-23 Hounsfield Units. In the case of missing CT scans at follow-up, the last observed edema volume was carried forward. All volumes were measured using Analyze 12.0 (Biomedical Imaging Resource, Mayo Clinic).[18]

Statistical Analyses

Diffusion indices in the edema or CST and contralateral regions were compared using two-way ANOVA. Differences in relative diffusion were tested with independent t-tests. Edema and hematoma volume changes were tested with the Wilcoxon signed rank test. FA depth data was compared with a One-Way ANOVA. Predictors of diffusion metrics were evaluated with linear regression or Spearman's correlation. Non-normally distributed hematoma and edema volumes were log-transformed prior to performing parametric statistical tests.

Results

Patient Characteristics

A total of 48 primary ICH patients were imaged with DTI. Twenty-seven patients were included in the current study after exclusions for the following reasons: previous CST lesion (n=7), ipsilateral CST did not overlap with edema (n=9), insufficient image quality, e.g. due to extreme movement (n=5). Patients were imaged at a median (interquartile range) of 2 (2) hours and 26 (28) hours with CT, and 42 (24) hours, and 8 (2) days with DTI. The majority of the patients received only a single scan, while 8 patients had DTI at both 72h and day 7. Clinical characteristics are listed in Table 5.1.

Table 5.1: Patient Characteristics

Age (mean±SD), y	67.7±13.4
Men	13 (48%)
Symptom onset to acute CT, h, median (IQR)	2.0 (1.8)
Symptom onset to 24h CT, h	25.9 (27.8)
Symptom onset to 72 hour DTI, h	42.3 (23.5)
Symptom onset to Day 7 DTI, d	7.7 (1.8)
Medical History	
Hypertension	15 (56%)
Previous stroke	2 (7%)
NIHSS total score	
Admission, n=26	13 (13)
72 Hours, n=23	15 (14)
Day 7, n=17	12 (14)
Day 90, n=20	6 (9)
NIHSS motor score	
Admission, n=26	3 (6)
72 Hours, n=24	3 (6)
Day 7, n=21	5 (7)
Day 90, n=23	2 (7)

DTI=Diffusion tensor imaging; d=day; h=hour; IQR=inter-quartile range; y=year; SD=standard deviation; and NIHSS=National Institute of Health Stroke Scale.

Hematoma distribution was: lobar 6 (22%), basal ganglia 13 (48%), thalamus 7 (26%) and brainstem 1 (4%). Median acute ICH volume was 8.8 (22) ml and increased to 14.8 (39.4) ml at 24 hours (p=0.004). Edema volume increased from 1.0 (2.6) ml acutely to 1.9 (3.9) ml at 24 hours (p=0.003). Absolute and relative diffusion values over time are listed in Tables 5.2-5.5.

Table 5.2: Absolute and Relative Fractional Anisotropy

Fractional Anisotropy, Mean±SD	
Edema FA, 72h	0.23±0.06
Edema FA, Day 7	0.22±0.04
Contralateral Edema FA, 72h	0.32±0.05
Contralateral Edema FA, Day 7	0.32±0.06
Edematous CST FA, 72h	0.37±0.03
Edematous CST FA, Day 7	0.35±0.08
Contralateral CST FA, 72h	0.52±0.06
Contralateral CST FA, Day 7	0.54±0.06
Relative Fractional Anisotropy	
Edema rFA, 72h	0.71±0.13
Edema rFA, Day 7	0.69±0.10
Edematous CST rFA, 72h	0.71±0.10
Edematous CST rFA, Day 7	0.64±0.14

CST = Corticospinal Tract; FA= Fractional Anisotropy; rFA= relative FA; SD= standard deviation.

Table 5.3: Absolute and Relative Mean Diffusivity

Mean Diffusivity, $x10^{-3}$ mm^2/s, Mean±SD	
Edema MD, 72h	1.1±0.12
Edema MD, Day 7	1.1±0.12
Contralateral Edema MD, 72h	0.91±0.11
Contralateral Edema MD, Day 7	0.89±0.13
Edematous CST MD, 72h	0.93±0.13
Edematous CST MD, Day 7	0.93±0.15
Contralateral CST MD, 72h	0.77±0.07
Contralateral CST MD, Day 7	0.75±0.07
Relative Mean Diffusivity	
Edema rMD, 72h	1.2±0.13
Edema rMD, Day 7	1.2±0.15
Edematous CST rMD, 72h	1.2±0.18
Edematous CST rMD, Day 7	1.2±0.23

CST = Corticospinal Tract; MD= Mean Diffusivity; rMD= relative MD; SD= standard deviation.

Table 5.4: Absolute and Relative Axial Diffusion

Axial Diffusion, $x10^{-3}$ mm^2/s, Mean±SD	
Edema AD, 72h	1.4±0.11
Edema AD, Day 7	1.3±0.13
Contralateral Edema AD, 72h	1.2±0.11
Contralateral Edema AD, Day 7	1.2±0.10
Edematous CST AD, 72h	1.3±0.18
Edematous CST AD, Day 7	1.3±0.21
Contralateral CST AD, 72h	1.3±0.15
Contralateral CST AD, Day 7	1.3±0.16
Relative Axial Diffusion	
Edema rAD, 72h	1.1±0.09
Edema rAD, Day 7	1.1±0.11
Edematous CST rAD, 72h	1.0±0.18
Edematous CST rAD, Day 7	1.0±0.22

AD = Axial Diffusion; CST = Corticospinal Tract; rAD= relative AD;

SD= standard deviation.

Table 5.5: Absolute and Relative Radial Diffusion

Radial Diffusion (RD), $x10^{-3}$ mm^2/s	
Edema RD, 72h	0.98±0.13
Edema RD, Day 7	0.97±0.12
Contralateral Edema RD, 72h	0.76±0.13
Contralateral Edema RD, Day 7	0.75±0.14
Edematous CST RD, 72h	0.73±0.10
Edematous CST RD, Day 7	0.74±0.14
Contralateral CST RD, 72h	0.51±0.04
Contralateral CST RD, Day 7	0.49±0.05
Relative Radial Diffusion (rRD)	
Edema rRD, 72h	1.3±0.18
Edema rRD, Day 7	1.3±0.20
Edematous CST rRD, 72h	1.4±0.22
Edematous CST rRD, Day 7	1.5±0.29

CST = Corticospinal Tract; RD= Radial Diffusion; rRD= relative RD; SD= standard deviation.

Perihematoma Edema Diffusion Changes Over Time

Diffusion was significantly different between the perihematoma edema and contralateral mirror region for FA, MD, AD and RD (all $p<0.0001$). FA was decreased in the edema (0.23±0.06) compared to contralateral tissue (0.32±0.05) at 72h. FA was also decreased in the edema (0.22±0.04) vs. contralateral tissue (0.32±0.06) at day 7 (Figure 5.2A). MD was increased in the

edema (1.1±0.12 x10^{-3} mm^2/s) compared to the contralateral tissue (0.91±0.11 x10^{-3} mm^2/s) at 72h and day 7 (edema: 1.1±0.12 x10^{-3} mm^2/s vs. contralateral tissue: 0.89±0.13 x10^{-3} mm^2/s, Figure 5.2B). AD was increased in the perihematoma edema (1.4±0.11 x10^{-3} mm^2/s) compared to contralateral tissue at 72h (1.3±0.18 x10^{-3} mm^2/s). At day 7, AD in the perihematoma edema was also increased (1.3±0.13 x10^{-3} mm^2/s) compared to contralateral tissue (vs 1.2±0.10 x10^{-3} mm^2/s; Figure 2C). Similarly, 72h RD values were higher in edema (0.98±0.13 x10^{-3} mm^2/s) compared to contralateral tissue (0.76±0.13 x10^{-3} mm^2/s). At Day 7 RD in the perihematoma edema (0.97±0.12 x10^{-3} mm^2/s) was also higher than the contralateral region (0.75±0.14 x10^{-3} mm^2/s; Figure 5.2D).

There was no change in diffusion in the perihematoma edema tissue between time-points for FA (p=0.933), MD (p=0.448), AD (p=0.293), or RD (p=0.583).

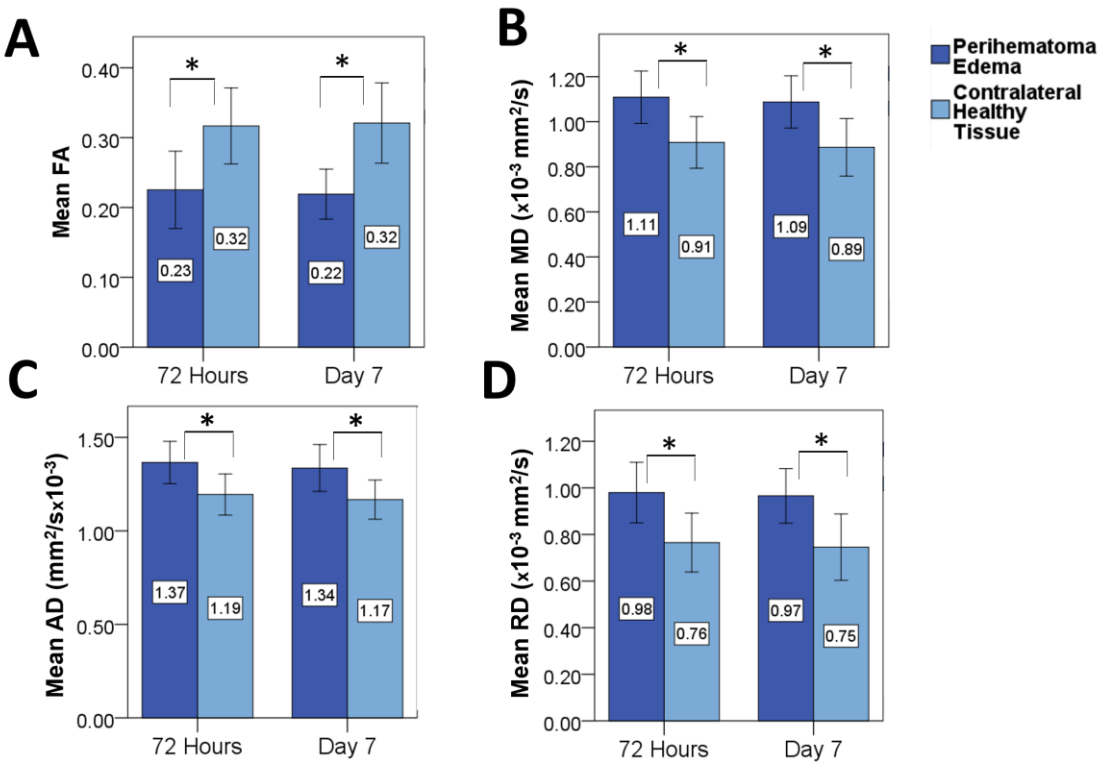

Figure 5.2. Diffusion metrics in the perihematoma edema and contralateral healthy tissue over time. Diffusion was significantly different between the two regions at both 72h and day 7. AD=Axial Diffusion; FA= Fractional Anisotropy; MD= Mean Diffusivity; RD= Radial Diffusion.

Mean Diffusion in the CST, Contralateral Tract, and Perihematoma Edema

There was a significant difference in diffusion values between the edema, the edematous CST, and the contralateral healthy tract for FA, MD, and RD (all $p<0.0001$). Only mean AD was not significantly different between the 3 regions ($p=0.111$).

FA in the tract passing through edema was increased at 72h (0.37±0.03) compared to perihematoma edema FA (0.23±0.06), and decreased relative to the contralateral tract (0.52±0.06). At day 7 FA in the tract through the edema (0.32±0.06) was also increased relative to edema (0.22±0.04) and decreased compared to the contralateral tract (0.54±0.06; Figure 5.3A).

FA in the 8 patients with consecutive 72h and day 7 scans was also significantly different between the edematous CST (0.37±0.03), the perihematoma edema (0.21±0.04) and the contralateral CST (0.52±0.08; $p<0.0001$ for all) at 72h, and at day 7 (edematous CST: 0.35±0.07, perihematoma edema: 0.24±0.03, contralateral CST: 0.55±0.08; $p<0.0001$).

At 72h, MD in the perihematoma edema (1.1±0.12 $x10^{-3}$ mm^2/s) was higher than MD in the edematous CST (0.93±0.13 $x10^{-3}$ mm^2/s), which was increased compared to the contralateral tract (0.77±0.07 $x10^{-3}$ mm^2/s). This pattern continued at Day 7 for MD in the edema (1.1±0.12 $x10^{-3}$ mm^2/s), the edematous CST (0.93±0.15 $x10^{-3}$ mm^2/s), and the contralateral CST (0.75±0.07 $x10^{-3}$ mm^2/s; Figure 5.3B).

AD in the edema at 72h (1.4±0.11 $x10^{-3}$ mm^2/s) was not different from AD in the edematous CST (1.3±0.18 $x10^{-3}$ mm^2/s) or in the contralateral tract (1.3±0.15 $x10^{-3}$ mm^2/s). Similarly, AD at day 7 did not change between locations (edema: 1.3±0.13 $x10^{-3}$ mm^2/s, edematous CST: 1.3±0.21 $x10^{-3}$ mm^2/s, contralateral CST: 1.3±0.16 $x10^{-3}$ mm^2/s; Figure 5.3C).

Perihematoma edema RD at 72h was increased (0.98±0.13 $x10^{-3}$ mm^2/s) compared to the edematous CST (0.73±0.10 $x10^{-3}$ mm^2/s), which was higher than RD in the contralateral tract (0.51±0.04 $x10^{-3}$ mm^2/s). The relationship between regions was maintained at day 7 (edema: 0.97±0.12 $x10^{-3}$ mm^2/s, edematous CST: 0.74±0.14 $x10^{-3}$ mm^2/s, contralateral CST: 0.49±0.05

x10^{-3} mm^2/s; Figure 5.3D).

All diffusion parameters remained stable over time: FA (p=0.745), MD (p=0.543), AD (p=0.499), and RD (p=0.677; Figure 5.3).

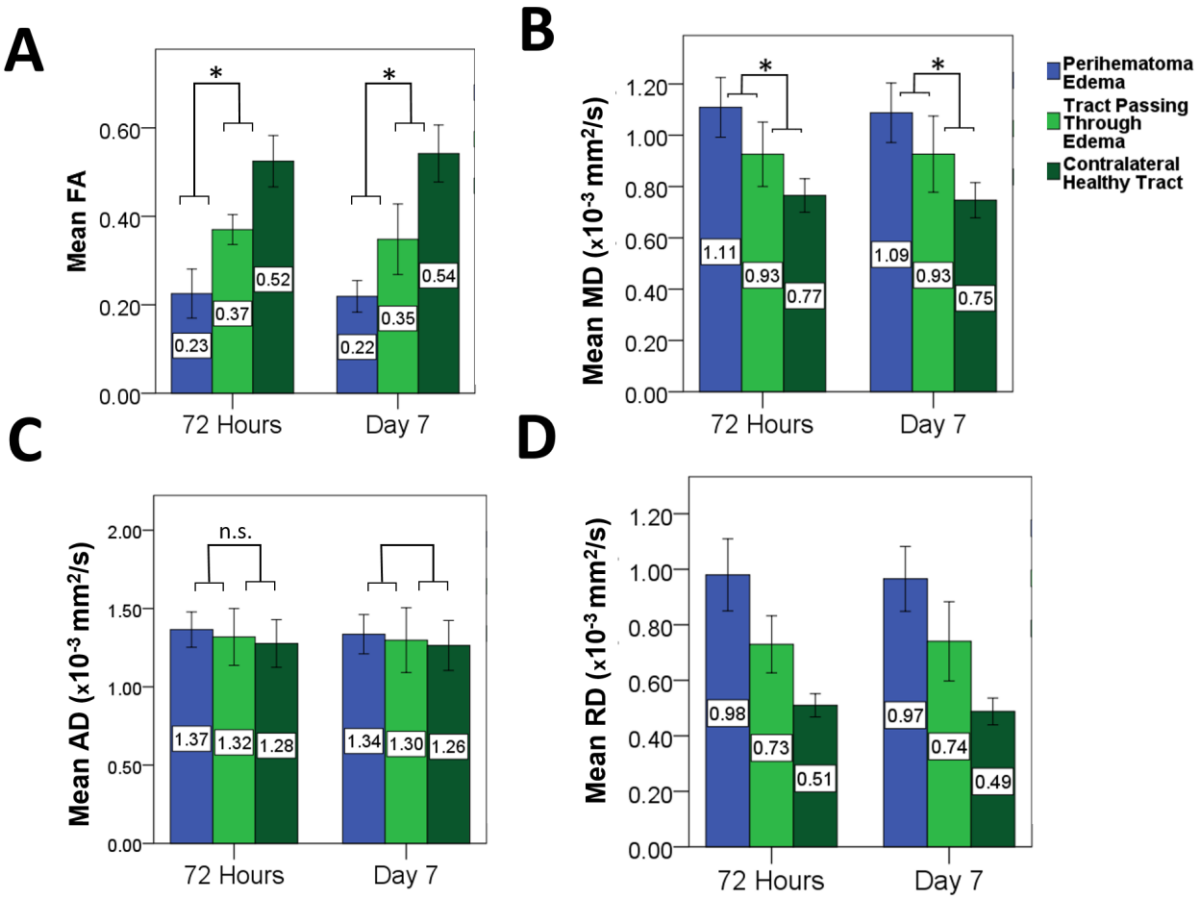

Figure 5.3. Comparison of diffusion metrics in the edematous Corticospinal Tract (CST), perihematoma edema and contralateral CST. The edematous CST diffusion was significantly different from that in the perihematoma edema and contralateral CST, with the exception of axial diffusion (AD). FA=Fractional Anisotropy; MD=Mean Diffusivity; RD=Radial Diffusion.

Diffusion and Edema Volume

Edema volume did not predict diffusion indices in the edematous CST at any time-point. Relative FA at 72h (β=-0.35, [-0.08- -0.01]; p=0.158) and day 7 (β=-0.28, [-0.09-0.03]; p=0.276) was not related to 24h edema volume.

Relative MD in the edematous CST was not related to 24h edema volume at 72h (β=-0.37, [-0.14-0.01]; p=0.129) or day 7 (β=0.11, [-0.08-0.12]; p=0.675).

24h edema volume was not predictive of rAD at 72h (β=-0.41, [-0.14-0.01]; p=0.091) or day 7 (β=0.05, [-0.09-0.11]; p=0.872) or rRD at 72h (β=-0.25, [-0.15-0.05]; p=0.319) or day 7 (β=0.013, [-0.10-0.17]; p=0.624).

Diffusion and Motor Score

There was no relationship between rFA, rMD, rAD or rRD in the edematous CST and 90-day NIHSS motor score (Table 5.6), or motor score at any other time.

Table 5.6: Association between Relative Diffusion and NIHSS Motor Score

	Day 90 NIHSSS Motor Score	
	ρ	p-value
rFA		
72 Hours	-0.22	0.420
Day 7	-0.14	0.624
rMD		
72 Hours	-0.31	0.251
Day 7	-0.31	0.275
rAD		
72 Hours	-0.40	0.125
Day 7	-0.30	0.290
rRD		
72 Hours	-0.25	0.352
Day 7	-0.05	0.875

AD=Axial Diffusion; FA=Fractional Anisotropy; MD=Mean Diffusivity; NIHSS=National Institute of Health; r=Relative; RD=Radial Diffusion

FA and Tract Depth Within the Perihematoma Edema

FA in the edematous CST was similar within the perihematoma edema, whether measured at the surface or center of the edema mask. FA in the edematous CST at a depth of 1 voxel into the edema mask (0.34±0.06, n=36) was not significantly different from FA at a depth of 2 voxels (0.32±0.06, n=30; p=0.876) or ≥3 voxels (0.30±0.10, n=21; p=0.127; Figure 5.4).

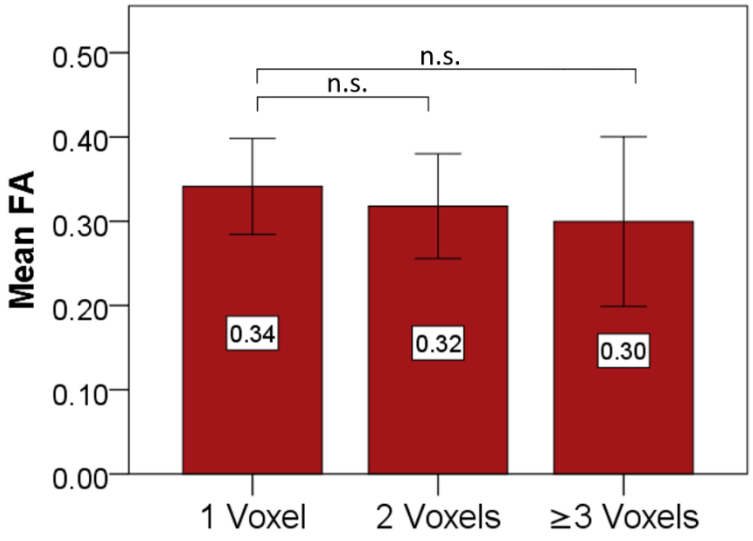

Figure 5.4. Fractional Anisotropy (FA) in the edematous Corticospinal Tract (CST) at different depths from the surface of the edema mask. FA was statistically similar between each category of voxels.

Discussion

We have shown that FA in the CST is decreased where it passes through edema, though not to the extent of the decrease observed in the surrounding perihematoma edema. The FA decrease remained stable over time, did not correlate with motor impairment, and likely represents water infiltration into the CST rather than decreased tract integrity.

Measuring Anisotropy within the Edema

FA in the edematous CST was measured and compared in different regions of the edema ROI, in order to confirm that measurements were not contaminated by inclusion of the hematoma. FA in surface voxels of the edematous CST was consistent with FA in deep voxels. There was no difference in edematous CST FA at 1, 2, or ≥3 voxels from the edema surface (Figure 5.4). This

suggests that edema ROIs correctly distinguished between edema and non-edema tissue at the border of the edema mask, where misclassification and PVE was most likely to affect FA measurement.

Diffusion in the Perihematoma Edema Region

FA was decreased and MD increased in the perihematoma edema compared to contralateral healthy tissue. Both radial and axial diffusion were also increased in the perihematoma edema (Figure 5.2). The reduction in directionality, and increase in diffusion, likely reflects the increased water content in edematous tissue.

Diffusion in the Edematous CST

We demonstrate that FA in the edematous CST is decreased relative to the contralateral CST at both 72h and day 7, but is increased relative to the surrounding perihematoma edema. All measured diffusion metrics in the edematous CST were intermediate to values in the contralateral CST and perihematoma edema (except AD, which was not affected; Figure 5.3).

FA is a sensitive measure of the progression of Wallerian degeneration.[19,20] Decreases in FA after CST injury are well documented,[21–23] have been observed as early as the first day of ICH,[24] and decrease with progression of tract degeneration.[25] A longitudinal study of diffusion in transected cat white matter found that FA decreased steadily from day 2-8.[20] FA has also been shown to decrease after ICH in patients whose diminished CST integrity is reflected clinically as poor motor outcome scores.[24,25] Contrary to what is expected in CST injury, FA in our study did not decrease between 72h and day 7. The stable reduction in FA and increase in MD are consistent with diffusion changes that would occur with increased water infiltration into the tracts, and suggest that CST integrity within the edematous CST is preserved.

Axial and Radial Diffusion in the Edematous CST

Axial and radial diffusion measurements reflect diffusion parallel and perpendicular to the tract, respectively, and provide insight into the underlying changes that affect FA.[15] We found that AD in the edematous CST did not vary with time or between locations. RD was increased in the edematous CST relative to the contralateral CST. Increases in RD have been observed in acute Wallerian degeneration, and in the presence of dysmyelination.[20,26,27] Increases are thus often regarded as a marker of tract injury. It is thus possible that tract integrity is decreased within the perihematoma edema, possibly secondary to injury from the nearby hematoma.

However, FA, RD and AD can also reflect non-pathological changes in microstructure. Decreased FA with correspondingly increased RD and unchanging AD has been previously noted in the presence of decreased axonal packing density.[28] Our results are also consistent with the hypothesis that hematoma-derived plasma infiltrates the CST, increasing the space between fibers and simultaneously increasing the diffusion perpendicular to the axons. As water diffusion becomes less directional in the increased space, anisotropy is correspondingly decreased.

Motor Scores and Edema Volumes

Diffusion changes in the edematous CST were not related to motor scores at day 90. Previous studies have shown that prediction of motor outcome after ICH is highly dependent on where CST diffusion is measured. In these studies, FA in the cerebral peduncle has consistently surpassed the predictive ability of other regions of the CST, including regions along the tract closer to the hematoma.[29,30] This counterintuitive finding is likely because the peduncle is distal to the lesion site and is therefore a more suitable location for detecting Wallerian degeneration, while the tract adjacent to the hematoma is likely to have decreased FA due to the surrounding

perihematoma edema.

Only one previous study has measured FA in the edematous CST.[31] FA was measured at 7±5 days, using a single small ROI placed in the region where the CST passed through the edema. Similar to our findings, rFA in this region was 0.6±0.03, lower than rFA in any other region of the CST. Edematous CST FA was not predictive of motor outcome.[31] However, the lack of controls, single time-point and lack of AD/RD measurements made it difficult to determine the integrity of the edematous CST compared to other ipsilateral regions.

Limitations

This study is limited by our relatively small dataset. The majority of our patients did not have consecutive DTI scans, thus limiting our ability to reliably measure changes in diffusion over time. However, secondary analyses of a smaller group of 8 patients with longitudinal data confirmed the findings of the larger cross-sectional comparisons.

In addition, the area of edema-tract overlap often consisted of only a few voxels, leaving the measurement prone to rater error. In order to confirm the validity of the edema ROI placement and to guard against contamination by hematoma FA, tract FA was measured and compared at multiple depths of edema, and was shown not to differ even at the border regions where measurement precision is decreased.

Finally, our imaging schedule includes assessment of edema within the first week after hemorrhage, when edema volume is at a peak. However, it is possible that a relationship between measures of tract integrity and edema develops beyond the period that we imaged patients post-ICH.

Conclusions

In this cross-sectional, prospective study, we found that FA is decreased in the CST where it passes through the perihematoma edema. The observed FA decrease remained stable over time, rather than decreasing as would be expected in a disintegrating tract. RD is increased in the edematous CST, indicating that diffusion perpendicular to axons is increased. These diffusion changes may reflect Wallerian degeneration in the CST due to the effect of the hematoma, however, they may also reflect increased spacing between axons as edema infiltrates. Neither the decreased FA or increased RD in the edematous CST was related to motor scores at 90 days post-ICH. Our results support the hypothesis that decreased FA in the edematous CST represents water infiltration into the CST, rather than tract impairment.

References

1. Grysiewicz, R. A., Thomas, K. & Pandey, D. K. Epidemiology of ischemic and hemorrhagic stroke: incidence, prevalence, mortality, and risk factors. *Neurol. Clin.* **26,** 871–95, vii (2008).

2. Chiu, D. *et al.* Comparison of Outcomes after Intracerebral Hemorrhage and Ischemic Stroke. *J. Stroke Cerebrovasc. Dis.* **19,** 225–229 (2010).

3. Broderick, J. P. *et al.* Guidelines for the Management of Spontaneous Intracerebral Hemorrhage : A Statement for Healthcare Professionals From a Special Writing Group of the Stroke Council, American Heart Association. *Stroke* **30,** 905–915 (1999).

4. Xi, G., Keep, R. F. & Hoff, J. T. Mechanisms of brain injury after intracerebral haemorrhage. *Lancet Neurology* **5,** 53–63 (2006).

5. Wasserman, J. K. & Schlichter, L. C. White matter injury in young and aged rats after intracerebral hemorrhage. *Exp. Neurol.* **214,** 266–275 (2008).

6. Barratt, H. E., Lanman, T. A. & Carmichael, S. T. Mouse intracerebral hemorrhage models produce different degrees of initial and delayed damage, axonal sprouting, and recovery. *J. Cereb. Blood Flow Metab.* **34,** 1463–71 (2014).

7. Wagner, K. R. *et al.* Lobar Intracerebral Hemorrhage Model in Pigs. *Stroke* **27,** 490–497 (1996).

8. Xi, G. *et al.* Role of Blood Clot Formation on Early Edema Development After Experimental Intracerebral Hemorrhage. *Stroke* **29,** 2580–2586 (1998).

9. Zazulia, A. R., Videen, T. O., Diringer, M. N. & Powers, W. J. Poor correlation between perihematomal MRI hyperintensity and brain swelling after intracerebral hemorrhage. *Neurocrit. Care* **15,** 436–41 (2011).

10. Mayer, S. a. *et al.* Perilesional Blood Flow and Edema Formation in Acute Intracerebral Hemorrhage : A SPECT Study. *Stroke* **29,** 1791–1798 (1998).

11. Olivot, J.-M. M. *et al.* MRI profile of the perihematomal region in acute intracerebral hemorrhage. *Stroke* **41,** 2681–2683 (2010).

12. Schellinger, P. D. *et al.* Stroke MRI in intracerebral hemorrhage: is there a perihemorrhagic penumbra? *Stroke.* **34,** 1674–9 (2003).

13. Butcher, K. S. *et al.* Perihematomal edema in primary intracerebral hemorrhage is plasma derived. *Stroke* **35,** 1879–1885 (2004).

14. Butcher, K. S. *et al.* The Intracerebral Hemorrhage Acutely Decreasing Arterial Pressure Trial. *Stroke.* **44,** 620–6 (2013).

15. Neil, J. J. Diffusion imaging concepts for clinicians. *J. Magn. Reson. Imaging* **27,** 1–7 (2008).

16. Rorden, C., Karnath, H.-O. & Bonilha, L. Improving lesion-symptom mapping. *J. Cogn. Neurosci.* **19,** 1081–1088 (2007).

17. Leemans, A., Jeurissen, B., Sijbers, J. & Jones, D. ExploreDTI: a graphical toolbox for processing, analyzing, and visualizing diffusion MR data. in *Proceedings 17th Scientific Meeting, International Society for Magnetic Resonance in Medicine* **17,** 3537 (2009).

18. Robb, R. A. *et al.* ANALYZE: A comprehensive, operator-interactive software package for multidimensional medical image display and analysis. *Comput. Med. Imaging Graph.* **13,** 433–454 (1989).

19. Thomalla, G. *et al.* Diffusion tensor imaging detects early Wallerian degeneration of the pyramidal tract after ischemic stroke. *Neuroimage* **22,** 1767–74 (2004).

20. Qin, W. *et al.* Wallerian degeneration in central nervous system: Dynamic associations between diffusion indices and their underlying pathology. *PLoS One* **7,** 1–10 (2012).

21. Wang, D.-M., Li, J., Liu, J.-R. & Hu, H.-Y. Diffusion tensor imaging predicts long-term motor functional outcome in patients with acute supratentorial intracranial hemorrhage. *Cerebrovasc. Dis.* **34,** 199–205 (2012).

22. Yokoyama, K. *et al.* Diffusion tensor imaging in chronic subdural hematoma: correlation between clinical signs and fractional anisotropy in the pyramidal tract. *AJNR. Am. J. Neuroradiol.* **29,** 1159–63 (2008).

23. Kusano, Y. *et al.* Prediction of functional outcome in acute cerebral hemorrhage using diffusion tensor imaging at 3T: a prospective study. *AJNR. Am. J. Neuroradiol.* **30,** 1561–5 (2009).

24. Ma, C., Liu, A., Li, Z., Zhou, X. & Zhou, S. Longitudinal study of diffusion tensor imaging properties of affected cortical spinal tracts in acute and chronic hemorrhagic stroke. *J. Clin. Neurosci.* **21,** 1388–1392 (2014).

25. Kuzu, Y. *et al.* Prediction of motor function outcome after intracerebral hemorrhage using fractional anisotropy calculated from diffusion tensor imaging. *Cerebrovasc. Dis.* **33,** 566–573 (2012).

26. Song, S. *et al.* Dysmyelination Revealed through MRI as Increased Radial (but Unchanged Axial) Diffusion of Water. *NeuroImage* **1436,** 1429–1436 (2002).

27. Budde, M. D. & Annese, J. Quantification of anisotropy and fiber orientation in human brain histological sections. *Front. Integr. Neurosci.* **7,** 3 (2013).

28. Takahashi, M. *et al.* Magnetic resonance microimaging of intraaxonal water diffusion in live excised lamprey spinal cord. *Proc. Natl. Acad. Sci. U. S. A.* **99,** 16192–6 (2002).

29. Tao, W.-D., Wang, J., Schlaug, G., Liu, M. & Selim, M. H. A Comparative Study of Fractional Anisotropy Measures and ICH Score in Predicting Functional Outcomes After Intracerebral Hemorrhage. *Neurocrit. Care* **21,** 417–25 (2014).

30. Koyama, T. *et al.* Diffusion tensor imaging for intracerebral hemorrhage outcome prediction: comparison using data from the corona radiata/internal capsule and the cerebral peduncle. *J. Stroke Cerebrovasc. Dis.* **22,** 72–9 (2013).

31. Cheng, C.-Y. *et al.* Motor outcome of deep intracerebral haemorrhage in diffusion tensor imaging: Comparison of data from different locations along the corticospinal tract. *Neurol. Res.* **37,** 774–781 (2015).

Chapter 6: Conclusions

The goal of this thesis was to provide insight into the mechanism of corticospinal tract (CST) injury after Intracerebral Hemorrhage (ICH). We sought to evaluate the relationship between the hematoma, patient outcome, and impairment of the CST. We also aimed to evaluate the effect of perihematoma edema on CST integrity. Both analyses were performed using Diffusion Tensor Imaging (DTI), a novel technique that allows estimation of tract integrity at a microstructural level. DTI provides a unique opportunity to evaluate microstructural changes in white matter after ICH, non-invasively and in-vivo. DTI metrics include Fractional Anisotropy (FA), a proxy for white matter integrity, Mean Diffusivity (MD), the average diffusion displacement, Axial Diffusivity (AD), which describes diffusion displacement parallel to the axon, and Radial Diffusivity (RD), which is diffusion displacement perpendicular to the axon.

There are few previous DTI studies relating CST integrity to hematoma volume[1–3] and only one that examined the relationship with perihematoma edema.[2] These studies had only one DTI time-point, which limited their ability to comment on the effect of edema and hematoma over time. Additionally, they did not incorporate measures of RD and AD, which are correlated with myelin and axon integrity, respectively, and can be used to infer the state of white matter integrity. Thus we are the first study to assess the longitudinal relationship between white matter integrity of the CST and hematoma/edema volumes, using FA, MD, RD and AD.

Hematoma Volume and CST Integrity

Acute hematoma volume is a significant predictor of outcome in ICH. Damage to the CST is common after ICH and is associated with motor impairment. However, few studies have explored the relationship between hematoma volume and CST integrity in vivo, as measured with DTI.

In order to address this gap in the literature, we tested the relationship between hematoma volume and diffusion metrics (FA, MD, AD and RD) measured in the CST at 72h, day 7 and day 30 post-stroke. We found that FA was decreased and RD increased in the ipsilateral CST, suggesting reduced tract integrity. We also found that larger hematoma volume predicted changes in FA and RD at day 30. This suggests that a pathological change in myelin integrity is occurring and is worsened with larger hemorrhages. The lack of association with diffusion at earlier time points and failure to observe consistent prediction of motor outcome with DTI are potentially due to the method of averaging diffusion along the entire CST.

While hemorrhage volume remains the more clinically useful metric for assessing post-ICH mortality and morbidity, we show that diffusion tensor imaging can be used to assess the specific relationship between volume and motor function. In particular, increased hematoma volume predicted decreased tract integrity in patient CSTs at day 30. These findings suggest that hematoma volume is a mediating factor in white matter change after ICH.

Edema and CST Integrity

Perihematoma edema is associated with intracerebral hemorrhage, however, it is unclear whether it is benign or represents a region of tissue injury.[4–8] DTI can be used to assess changes in diffusion in white matter that may indicate a deleterious effect of edema. One previous study has observed decreased FA in white matter within edema,[2] however, their measurement technique was imprecise, imaging was restricted to one time-point, and they lacked an analysis of AD and RD.

Our goal was to perform a study that addressed these limitations in order to assess the relationship between perihematoma edema and CST integrity in ICH. We measured diffusion in the region of the CST where it passes through the edema (the ‘edematous CST’). Diffusion in the

edematous CST was assessed at multiple time-points (72h and day 7). We found that FA was decreased and RD was increased in the CST where it passes through edema, though not to the extent of the decrease observed in the surrounding perihematoma edema. These changes may be indicative of white matter impairment following ICH. However, RD and FA remained stable over time, and did not correlate with motor impairment. Taken together, these results suggest diffusion changes that reflect the increased water content in the edematous tissue. Our results support the hypothesis that diffusion changes in the edematous CST represent water infiltration into the CST, rather than tract impairment.

Strengths and Limitations

Strengths

These studies contribute new information to the current literature on diffusion in the CST after ICH. In particular, we provide unique analysis of RD and AD in the CST, and are the first to report those values within the edematous CST. Measurements of RD and AD provide a more complete picture of the state of diffusion than can be obtained simply with FA.[9]

Our study had a number of methodological strengths. The measurements of hematoma and edema volume were performed planimetrically, and thus are more precise than commonly used methods of estimating volume.[10] We are the only study to measure diffusion specifically in the region where the CST passes through the edema, resulting in a very precise, voxel-based measurement.

We evaluated diffusion metrics at 72h, day 7 and day 30, allowing an assessment of FA changes over time. Very few previous studies of FA in the CST after ICH used more than one time-point.[11,12]

Limitations

This study is limited by our relatively small dataset. In addition, our goal of obtaining longitudinal data was hindered by the natural complications of obtaining serial imaging in a group of patients with high mortality and morbidity. As a result, few patients had true serial imaging, and we were forced to limit our analysis to small groups of patients who had two consecutive scans. This doubtless influenced our ability to get a picture of changes in diffusion over time.

Though averaging diffusion along the entire tract provided a good estimate of whole-tract diffusion, the disadvantage was that it also averaged across multiple regions of diffusion changes within the CST. This likely affected our ability to find a strongly predictive relationship between DTI metrics and motor outcome, and also to observe significant changes in FA over time.

Closing Remarks

This research contributes to the understanding of integrity of the CST following ICH.

We used DTI to assess changes in the CST in-vivo. DTI studies have an advantage over histological analyses in that they provide data in-vivo, so that changes over time, and in relation to motor outcome, can be assessed concomitantly. However, DTI is inferior to histology in that it can only indirectly assess changes in tract structure. Our study provides information about how the hematoma and perihematoma edema affect the CST in live patients. This data contributes to an understanding of the state of the CST after ICH, which may in turn inform studies aimed at prevention and treatment. Assessment of the function of the CST with DTI could be useful in informing decision making regarding end of life care and rehabilitation. DTI is not routinely used clinically at present, however, more and more studies on its prognostic value in ICH are

appearing in the literature.[13,14] Thus, our data also serves to inform future studies of diffusion in white matter after ICH.

Recommended Directions for Future Studies

Based on our findings, we have a number of methodological recommendations for future studies of ICH.

First, it is preferable not to average diffusion throughout the entire CST if the goal of the study is to predict outcome. Instead, measure diffusion in regions that are expected to experience more Wallerian degeneration and therefore best reflect motor function. Previous studies have had success with FA evaluations in the cerebral peduncles.[1,12,15–17]

Secondly, evaluate FA changes over time in the context of motor outcome. This will help to prevent group analysis results from averaging across the reciprocal changes expected in patients with good vs. poor outcome.

Third, it is highly recommended that future studies include measurements of radial and axial diffusion. These values help to ascertain the profile of diffusion that underlies changes in FA, and can contribute valuable information to analysis of microstructure. RD and AD are reported in ischemic diffusion literature but are perplexingly absent in ICH-DTI studies to date.

Finally, our results reflect the complexity of imaging white matter in the perihematoma region. Both pathological and non-pathological factors in this area can affect diffusion. In particular, future studies investigating integrity of the CST in proximity to hemorrhage should be aware of the potentially confounding effect of edema on diffusion measurement.

References

1. Koyama, T., Marumoto, K., Miyake, H., Ohmura, T. & Domen, K. Relationship between diffusion-tensor fractional anisotropy and long-term outcome in patients with hemiparesis after intracerebral hemorrhage. *NeuroRehabilitation* **32,** 87–94 (2013).

2. Cheng, C.-Y. *et al.* Motor outcome of deep intracerebral haemorrhage in diffusion tensor imaging: Comparison of data from different locations along the corticospinal tract. *Neurol. Res.* **37,** 774–781 (2015).

3. Yoshioka, H. *et al.* Diffusion tensor tractography predicts motor functional outcome in patients with spontaneous intracerebral hemorrhage. *Neurosurgery* **62,** 97–103; discussion 103 (2008).

4. Wagner, K. R. *et al.* Lobar Intracerebral Hemorrhage Model in Pigs. *Stroke* **27,** 490–497 (1996).

5. Xi, G. *et al.* Role of Blood Clot Formation on Early Edema Development After Experimental Intracerebral Hemorrhage. *Stroke* **29,** 2580–2586 (1998).

6. Zazulia, A. R., Videen, T. O., Diringer, M. N. & Powers, W. J. Poor correlation between perihematomal MRI hyperintensity and brain swelling after intracerebral hemorrhage. *Neurocrit. Care* **15,** 436–41 (2011).

7. Olivot, J.-M. M. *et al.* MRI profile of the perihematomal region in acute intracerebral hemorrhage. *Stroke* **41,** 2681–2683 (2010).

8. Butcher, K. S. *et al.* Perihematomal edema in primary intracerebral hemorrhage is plasma derived. *Stroke* **35,** 1879–1885 (2004).

9. Mori, S. & Zhang, J. Principles of Diffusion Tensor Imaging and Its Applications to Basic Neuroscience Research. *Neuron* **51,** 527–539 (2006).

10. Kothari, R. U. *et al.* The ABCs of measuring intracerebral hemorrhage volumes. *Stroke.* **27,** 1304–1305 (1996).

11. Ma, C., Liu, A., Li, Z., Zhou, X. & Zhou, S. Longitudinal study of diffusion tensor imaging properties of affected cortical spinal tracts in acute and chronic hemorrhagic stroke. *J. Clin. Neurosci.* **21,** 1388–1392 (2014).

12. Kuzu, Y. *et al.* Prediction of motor function outcome after intracerebral hemorrhage using fractional anisotropy calculated from diffusion tensor imaging. *Cerebrovasc. Dis.* **33,** 566–573 (2012).

13. Kumar, P., Kathuria, P., Nair, P. & Prasad, K. Prediction of Upper Limb Motor Recovery after Subacute Ischemic Stroke Using Diffusion Tensor Imaging : A Systematic Review and Meta-Analysis. *JOS* **18,** 50–59 (2016).

14. Buerger, K. *et al.* Preditcing Motor Improvement After Stroke: Assessment and Diffusion Tensor Imaging. *Neurology* **181,** 6–7 (2005).

15. Wang, D.-M., Li, J., Liu, J.-R. & Hu, H.-Y. Diffusion tensor imaging predicts long-term motor functional outcome in patients with acute supratentorial intracranial hemorrhage. *Cerebrovasc. Dis.* **34,** 199–205 (2012).

16. Kusano, Y. *et al.* Prediction of functional outcome in acute cerebral hemorrhage using diffusion tensor imaging at 3T: a prospective study. *AJNR. Am. J. Neuroradiol.* **30,** 1561–5 (2009).

17. Koyama, T. *et al.* Diffusion tensor imaging for intracerebral hemorrhage outcome prediction: comparison using data from the corona radiata/internal capsule and the cerebral peduncle. *J. Stroke Cerebrovasc. Dis.* **22,** 72–9 (2013).

Bibliography

1. Asdaghi, N., Manawadu, D. & Butcher, K. Therapeutic management of acute intracerebral haemorrhage. *Expert Opin. Pharmacother.* **8,** 3097–116 (2007).
2. Sacco, S., Marini, C., Toni, D., Olivieri, L. & Carolei, A. Incidence and 10-year survival of intracerebral hemorrhage in a population-based registry. *Stroke.* **40,** 394–9 (2009).
3. Grysiewicz, R. A., Thomas, K. & Pandey, D. K. Epidemiology of ischemic and hemorrhagic stroke: incidence, prevalence, mortality, and risk factors. *Neurol. Clin.* **26,** 871–95, vii (2008).
4. Foulkes, M. A. & others. The Stroke Data Bank: design, methods, and baseline characteristics. *Stroke* **19,** 547–554 (1988).
5. Linn, J. & Brückmann, H. Differential diagnosis of nontraumatic intracerebral hemorrhage. *Klin. Neuroradiol.* **19,** 45–61 (2009).
6. Qureshi, A. I. *et al.* Spontaneous Intracerebral Hemorrhage. *NEJM* **344,** 1450–1460 (2001).
7. Mutlu, N., RG, B. & BJ, A. Massive cerebral hemorrhage: Clinical and pathological correlations. *Arch. Neurol.* **8,** 644–661 (1963).
8. Sahni, R. & Weinberger, J. Management of intracerebral hemorrhage. *VHRM* **3,** 701–709 (2007).
9. Hemphill, J. C. *et al.* Guidelines for the Management of Spontaneous Intracerebral Hemorrhage: A Guideline for Healthcare Professionals from the American Heart Association/American Stroke Association. *Stroke* **46,** (2015).
10. Sridharan, S. E. *et al.* Incidence, types, risk factors, and outcome of stroke in a developing

country the trivandrum stroke registry. *Stroke* **40,** 1212–1218 (2009).

11. van Asch, C. J. *et al.* Incidence, case fatality, and functional outcome of intracerebral haemorrhage over time, according to age, sex, and ethnic origin: a systematic review and meta-analysis. *Lancet Neurol.* **9,** 167–76 (2010).
12. Magistris, F., Bazak, S. & Martin, J. Intracerebral Hemorrhage: Pathophysiology, Diagnosis and Management. *MUMJ* **10,** 15–22 (2000).
13. Sturgeon, J. D. *et al.* Risk factors for intracerebral hemorrhage in a pooled prospective study. *Stroke* **38,** 2718–2725 (2007).
14. Ariesen, M. J., Claus, S. P., Rinkel, G. J. E. & Algra, A. Risk factors for intracerebral hemorrhage in the general population: A systematic review. *Stroke* **34,** 2060–2065 (2003).
15. Ikram, M. A., Wieberdink, R. G. & Koudstaal, P. J. International epidemiology of intracerebral hemorrhage. *Curr. Atheroscler. Rep.* **14,** 300–6 (2012).
16. Hill, M. D., Silver, F. L., Austin, P. C. & Tu, J. V. Rate of stroke recurrence in patients with primary intracerebral hemorrhage. *Stroke.* **31,** 123–127 (2000).
17. Khan, N. a *et al.* Risk factors, quality of care and prognosis in South Asian, East Asian and White patients with stroke. *BMC Neurol.* **13,** 74 (2013).
18. Gebel, J. M. & Broderick, J. P. Intracerebral hemorrhage. *Neurol. Clin.* **18,** 419–38 (2000).
19. Broderick, J. P., Brott, T. G., Duldner, J. E., Tomsick, T. & Huster, G. Volume of intracerebral hemorrhage. A powerful and easy-to-use predictor of 30-day mortality. *Stroke.* **24,** 987–993 (1993).
20. Katrak, P. H., Black, D. & Peeva, V. Do stroke patients with intracerebral hemorrhage have a better functional outcome than patients with cerebral infarction? *PM & R* **1,** 427–

33 (2009).

21. Krishnamurthi, R. V. *et al.* Global and regional burden of first-ever ischaemic and haemorrhagic stroke during 1990-2010: Findings from the Global Burden of Disease Study 2010. *Lancet Glob. Heal.* **1,** (2013).

22. Broderick, J. P. *et al.* Guidelines for the Management of Spontaneous Intracerebral Hemorrhage. *Stroke* **30,** 905–915 (2015).

23. Gor-Garcia-Fogeda, D. *et al.* Scales to assess gross motor function in stroke patients: A systematic review. *Arch. Phys. Med. Rehabil.* **95,** 1174–1183 (2014).

24. Xi, G., Keep, R. F. & Hoff, J. T. Mechanisms of brain injury after intracerebral haemorrhage. *Lancet Neurology* **5,** 53–63 (2006).

25. Barratt, H. E., Lanman, T. A. & Carmichael, S. T. Mouse intracerebral hemorrhage models produce different degrees of initial and delayed damage, axonal sprouting, and recovery. *J. Cereb. Blood Flow Metab.* **34,** 1463–71 (2014).

26. Wasserman, J. K. & Schlichter, L. C. White matter injury in young and aged rats after intracerebral hemorrhage. *Exp. Neurol.* **214,** 266–275 (2008).

27. Venkatasubramanian, C. *et al.* Natural history and prognostic value of corticospinal tract Wallerian degeneration in intracerebral hemorrhage. *JAHA* **2,** e000090 (2013).

28. Thomalla, G. *et al.* Diffusion tensor imaging detects early Wallerian degeneration of the pyramidal tract after ischemic stroke. *Neuroimage* **22,** 1767–1774 (2004).

29. Leira, R. *et al.* Early neurologic deterioration in intracerebral hemorrhage: predictors and associated factors. *Neurology* **63,** 461–7 (2004).

30. Brott, T. *et al.* Early hemorrhage growth in patients with intracerebral hemorrhage. *Stroke.* **28,** 1–5 (1997).

31. Wagner, K. R. *et al.* Lobar intracerebral hemorrhage model in pigs: rapid edema development in perihematomal white matter. *Stroke.* **27,** 490–497 (1996).

32. Xi, G. *et al.* Role of Blood Clot Formation on Early Edema Development After Experimental Intracerebral Hemorrhage. *Stroke* **29,** 2580–2586 (1998).

33. Zazulia, A. R., Videen, T. O., Diringer, M. N. & Powers, W. J. Poor correlation between perihematomal MRI hyperintensity and brain swelling after intracerebral hemorrhage. *Neurocrit. Care* **15,** 436–41 (2011).

34. Xi, G., Keep, R. F. & Hoff, J. T. Pathophysiology of brain edema formation. *Neurosurg Clin N Am* **13,** 371–383 (2002).

35. Butcher, K. S. *et al.* Perihematomal edema in primary intracerebral hemorrhage is plasma derived. *Stroke* **35,** 1879–1885 (2004).

36. Olivot, J.-M. M. *et al.* MRI profile of the perihematomal region in acute intracerebral hemorrhage. *Stroke* **41,** 2681–2683 (2010).

37. Butcher, K. S. *et al.* The Intracerebral Hemorrhage Acutely Decreasing Arterial Pressure Trial. *Stroke.* **44,** 620–6 (2013).

38. Carhuapoma, J. R., Hanley, D. F., Banerjee, M. & Beauchamp, N. J. Brain edema after human cerebral hemorrhage: a magnetic resonance imaging volumetric analysis. *J. Neurosurg. Anesthesiol.* **15,** 230–3 (2003).

39. Carhuapoma, J. R., Barker, P. B., Hanley, D. F., Wang, P. & Beauchamp, N. J. Human Brain Hemorrhage : Quantification of Perihematoma Edema by Use of Diffusion-Weighted MR Imaging. *AJNR* **23,** 1322–1326 (2002).

40. Urday, S. *et al.* Hemorrhage. *Stroke* **46,** 1–11 (2015).

41. Murthy, S. B. *et al.* Perihematomal Edema and Functional Outcomes in Intracerebral

Hemorrhage Influence of Hematoma Volume and Location. *Stroke* **46,** 1–12 (2015).

42. Fan, Y. & Lin, K. Changes in structural integrity are correlated with motor and functional recovery after post- stroke rehabilitation Changes in structural integrity are correlated with motor and functional recovery after post-stroke rehabilitation. *Rest. Neurol. and Neuro.* **33,** 835–844 (2015).

43. Gebel, J. M. *et al.* Relative Edema Volume Is a Predictor of Outcome in Patients With Hyperacute Spontaneous Intracerebral Hemorrhage. *Stroke* **33,** 2636–2641 (2002).

44. Arima, H. *et al.* Significance of perihematomal edema in acute intracerebral hemorrhage: the INTERACT trial. *Neurology* **73,** 1963–1968 (2009).

45. Butcher, K. & Emery, D. Acute stroke imaging. Part I: Fundamentals. *Can. J. Neurol. Sci.* **37,** 4–16 (2010).

46. Mori, S. & Zhang, J. Principles of diffusion tensor imaging and its applications to basic neuroscience research. *Neuron* **51,** 527–539 (2006).

47. Alexander, A. L., Lee, J. E., Lazar, M. & Field, A. S. Diffusion Tensor Imaging of the Brain. *Natl. Inst. Heal.* **4,** 316–329 (2008).

48. Neil, J. J. Diffusion imaging concepts for clinicians. *J. Magn. Reson. Imaging* **27,** 1–7 (2008).

49. Le Bihan, D. *et al.* Diffusion tensor imaging: concepts and applications. *J. Magn. Reson. Imaging* **13,** 534–46 (2001).

50. Beaulieu, C. The basis of anisotropic water diffusion in the nervous system - A technical review. *NMR Biomed.* **15,** 435–455 (2002).

51. Mori, S. & van Zijl, P. C. M. Fiber tracking: principles and strategies - a technical review. *NMR Biomed.* **15,** 468–80 (2002).

52. Qin, W. *et al.* Wallerian degeneration in central nervous system: Dynamic associations between diffusion indices and their underlying pathology. *PLoS One* **7,** 1–10 (2012).

53. Song, S.-K. *et al.* Dysmyelination Revealed through MRI as Increased Radial (but Unchanged Axial) Diffusion of Water. *Neuroimage* **17,** 1429–1436 (2002).

54. Budde, M. D. & Annese, J. Quantification of anisotropy and fiber orientation in human brain histological sections. *Front. Integr. Neurosci.* **7,** 3 (2013).

55. Cho, S. H. S.-H. *et al.* Motor outcome according to diffusion tensor tractography findings in the early stage of intracerebral hemorrhage. *Neurosci. Lett.* **421,** 142–6 (2007).

56. Yeo, S. S., Choi, B. Y., Chang, C. H. & Jang, S. H. Transpontine connection fibers between corticospinal tracts in hemiparetic patients with intracerebral hemorrhage. *Eur. Neurol.* **63,** 154–8 (2010).

57. Khalsa, S., Mayhew, S. D., Chechlacz, M., Bagary, M. & Bagshaw, A. P. The structural and functional connectivity of the posterior cingulate cortex: Comparison between deterministic and probabilistic tractography for the investigation of structure-function relationships. *Neuroimage* **102,** 118–127 (2014).

58. Hollocks, M. J. *et al.* Differential relationships between apathy and depression with white matter microstructural changes and functional outcomes. *Brain* **138,** 3803–3815 (2015).

59. Benders, M. J. N. L., Kersbergen, K. J. & de Vries, L. S. Neuroimaging of White Matter Injury, Intraventricular and Cerebellar Hemorrhage. *Clinics in Perinatology* **41,** 69–82 (2014).

60. Neeb, L. *et al.* No microstructural white matter alterations in chronic and episodic migraineurs: A case-control diffusion tensor magnetic resonance imaging study. *Headache* **55,** 241–251 (2015).

61. Wan, C. Y., Zheng, X., Marchina, S., Norton, A. & Schlaug, G. Intensive therapy induces contralateral white matter changes in chronic stroke patients with Broca's aphasia. *Brain Lang.* **136,** 1–7 (2014).

62. Yamada, Kei; Patel, Uresh; Shrier, David; Tanaka, Hisashi; Chang, Ja-Kwei; Numaguchi, Y. MR Imaging of CNS tractopathy: Wallerian and Transneural Degeneration. *AJR* **171,** 813–18 (1998).

63. Vargas, M. E. & Barres, B. A. Why Is Wallerian Degeneration in the CNS So Slow? *Annu. Rev. Neurosci.* **30,** 153–179 (2007).

64. Sawlani, V., Gupta, R. K., Singh, M. K. & Kohli, A. MRI demonstration of Wallerian degeneration in various intracranial lesions and its clinical implications. *J. Neurol. Sci.* **146,** 103–108 (1997).

65. Pierpaoli, C. *et al.* Water diffusion changes in Wallerian degeneration and their dependence on white matter architecture. *Neuroimage* **13,** 1174–85 (2001).

66. Kusano, Y. *et al.* Prediction of functional outcome in acute cerebral hemorrhage using diffusion tensor imaging at 3T: a prospective study. *AJNR. Am. J. Neuroradiol.* **30,** 1561–5 (2009).

67. Concha, L., Gross, D. W., Wheatley, B. M. & Beaulieu, C. Diffusion tensor imaging of time-dependent axonal and myelin degradation after corpus callosotomy in epilepsy patients. *Neuroimage* **32,** 1090–1099 (2006).

68. Kuzu, Y. *et al.* Prediction of motor function outcome after intracerebral hemorrhage using fractional anisotropy calculated from diffusion tensor imaging. *Cerebrovasc. Dis.* **33,** 566–573 (2012).

69. Ma, C., Liu, A., Li, Z., Zhou, X. & Zhou, S. Longitudinal study of diffusion tensor

imaging properties of affected cortical spinal tracts in acute and chronic hemorrhagic stroke. *J. Clin. Neurosci.* **21,** 1388–1392 (2014).

70. Koyama, T., Marumoto, K., Uchiyama, Y., Miyake, H. & Domen, K. Outcome assessment of hemiparesis due to intracerebral hemorrhage using diffusion tensor fractional anisotropy. *J. Stroke Cerebrovasc. Dis.* **24,** 881–889 (2015).

71. Koyama, T., Marumoto, K., Miyake, H., Ohmura, T. & Domen, K. Relationship between diffusion-tensor fractional anisotropy and long-term outcome in patients with hemiparesis after intracerebral hemorrhage. *NeuroRehabilitation* **32,** 87–94 (2013).

72. Koyama, T. *et al.* Diffusion tensor imaging for intracerebral hemorrhage outcome prediction: comparison using data from the corona radiata/internal capsule and the cerebral peduncle. *J. Stroke Cerebrovasc. Dis.* **22,** 72–9 (2013).

73. Wang, D.-M., Li, J., Liu, J.-R. & Hu, H.-Y. Diffusion tensor imaging predicts long-term motor functional outcome in patients with acute supratentorial intracranial hemorrhage. *Cerebrovasc. Dis.* **34,** 199–205 (2012).

74. Koyama, T., Tsuji, M., Miyake, H., Ohmura, T. & Domen, K. Motor outcome for patients with acute intracerebral hemorrhage predicted using diffusion tensor imaging: An application of ordinal logistic modeling. *J. Stroke Cerebrovasc. Dis.* **21,** 704–711 (2012).

75. Yoshioka, H. *et al.* Diffusion Tensor Tractography Predicts Motor Functional Outcome In Patients With Spontaneous Intracerebral Hemorrhage. *Neurosurgery* **62,** 97–103 (2008).

76. Yokoyama, K. *et al.* Diffusion tensor imaging in chronic subdural hematoma: correlation between clinical signs and fractional anisotropy in the pyramidal tract. *AJNR. Am. J. Neuroradiol.* **29,** 1159–63 (2008).

77. Yeo, S. S. *et al.* Periventricular white matter injury by primary intraventricular

hemorrhage: a diffusion tensor imaging study. *Eur. Neurol.* **66,** 235–41 (2011).

78. Yeo, S. S. *et al.* Evidence of corticospinal tract injury at midbrain in patients with subarachnoid hemorrhage. *Stroke.* **43,** 2239–41 (2012).

79. Cheng, C.-Y. *et al.* Motor outcome of deep intracerebral haemorrhage in diffusion tensor imaging: Comparison of data from different locations along the corticospinal tract. *Neurol. Res.* **37,** 774–781 (2015).

80. Kothari, R. U. *et al.* The ABCs of measuring intracerebral hemorrhage volumes. *Stroke.* **27,** 1304–1305 (1996).

81. Lee, K. B. *et al.* The motor recovery related with brain lesion in patients with intracranial hemorrhage. *Behav. Neurol.* **2015,** 258161 (2015).

82. Mori, S. & Zhang, J. Principles of Diffusion Tensor Imaging and Its Applications to Basic Neuroscience Research. 527–539 (2006). doi:10.1016/j.neuron.2006.08.012

83. Ma, C., Liu, A., Li, Z., Zhou, X. & Zhou, S. Longitudinal study of diffusion tensor imaging properties of affected cortical spinal tracts in acute and chronic hemorrhagic stroke. *J. Clin. Neurosci.* **21,** 1–5 (2014).

84. Robb, R. A. *et al.* ANALYZE: A comprehensive, operator-interactive software package for multidimensional medical image display and analysis. *Comput. Med. Imaging Graph.* **13,** 433–454 (1989).

85. Leemans, A., Jeurissen, B., Sijbers, J. & Jones, D. ExploreDTI: a graphical toolbox for processing, analyzing, and visualizing diffusion MR data. in *Proceedings 17th Scientific Meeting, International Society for Magnetic Resonance in Medicine* **17,** 3537 (2009).

86. Rorden, C., Karnath, H.-O. & Bonilha, L. Improving lesion-symptom mapping. *J. Cogn. Neurosci.* **19,** 1081–1088 (2007).

87. Hirai, K. K., Groisser, B. N., Copen, W. A., Singhal, A. B. & Schaechter, J. D. Comparing prognostic strength of acute corticospinal tract injury measured by a new diffusion tensor imaging based template approach versus common approaches. *J. Neurosci. Methods* **257,** 204–213 (2016).

88. Pantoni, L. *et al.* Impact of age-related cerebral white matter changes on the transition to disability - The LADIS study: Rationale, design and methodology. *Neuroepidemiology* **24,** 51–62 (2005).

89. Kosior, J. C. *et al.* Quantomo: validation of a computer-assisted methodology for the volumetric analysis of intracerebral haemorrhage. *Int. J. Stroke* **6,** 302–305 (2011).

90. Kuzu, Y. *et al.* Prediction of motor function outcome after intracerebral hemorrhage using fractional anisotropy calculated from diffusion tensor imaging. *Cerebrovasc. Dis.* **33,** 566–573 (2012).

91. Song, S. *et al.* Dysmyelination Revealed through MRI as Increased Radial (but Unchanged Axial) Diffusion of Water. *NeuroImage* **1436,** 1429–1436 (2002).

92. Beaulieu, C. & Allen, P. S. Determinants of anisotropic water diffusion in nerves. *Magn. Reson. Med.* **31,** 394–400 (1994).

93. Yoshioka, H. *et al.* Diffusion tensor tractography predicts motor functional outcome in patients with spontaneous intracerebral hemorrhage. *Neurosurgery* **62,** 97–103; discussion 103 (2008).

94. Ma, C., Liu, A., Li, Z., Zhou, X. & Zhou, S. Longitudinal study of diffusion tensor imaging properties of affected cortical spinal tracts in acute and chronic hemorrhagic stroke. *J. Clin. Neurosci.* **21,** 1388–1392 (2014).

95. Koyama, T., Marumoto, K., Miyake, H., Ohmura, T. & Domen, K. Relationship between

diffusion-tensor fractional anisotropy and long-term outcome in patients with hemiparesis after intracerebral hemorrhage. *NeuroRehabilitation* **32,** 87–94 (2013).

96. Tao, W.-D., Wang, J., Schlaug, G., Liu, M. & Selim, M. H. A Comparative Study of Fractional Anisotropy Measures and ICH Score in Predicting Functional Outcomes After Intracerebral Hemorrhage. *Neurocrit. Care* **21,** 417–25 (2014).

97. Chiu, D. *et al.* Comparison of Outcomes after Intracerebral Hemorrhage and Ischemic Stroke. *J. Stroke Cerebrovasc. Dis.* **19,** 225–229 (2010).

98. Broderick, J. P. *et al.* Guidelines for the Management of Spontaneous Intracerebral Hemorrhage : A Statement for Healthcare Professionals From a Special Writing Group of the Stroke Council, American Heart Association. *Stroke* **30,** 905–915 (1999).

99. Wagner, K. R. *et al.* Lobar Intracerebral Hemorrhage Model in Pigs. *Stroke* **27,** 490–497 (1996).

100. Mayer, S. a. *et al.* Perilesional Blood Flow and Edema Formation in Acute Intracerebral Hemorrhage : A SPECT Study. *Stroke* **29,** 1791–1798 (1998).

101. Schellinger, P. D. *et al.* Stroke MRI in intracerebral hemorrhage: is there a perihemorrhagic penumbra? *Stroke.* **34,** 1674–9 (2003).

102. Neil, J. J. Diffusion imaging concepts for clinicians. *J. Magn. Reson. Imaging* **27,** 1–7 (2008).

103. Thomalla, G. *et al.* Diffusion tensor imaging detects early Wallerian degeneration of the pyramidal tract after ischemic stroke. *Neuroimage* **22,** 1767–74 (2004).

104. Takahashi, M. *et al.* Magnetic resonance microimaging of intraaxonal water diffusion in live excised lamprey spinal cord. *Proc. Natl. Acad. Sci. U. S. A.* **99,** 16192–6 (2002).

105. Mori, S. & Zhang, J. Principles of Diffusion Tensor Imaging and Its Applications to Basic

Neuroscience Research. *Neuron* **51,** 527–539 (2006).

106. Kumar, P., Kathuria, P., Nair, P. & Prasad, K. Prediction of Upper Limb Motor Recovery after Subacute Ischemic Stroke Using Diffusion Tensor Imaging : A Systematic Review and Meta-Analysis. **18,** 50–59 (2016).

107. Buerger, K. *et al.* Preditcing Motor Improvement After Stroke: Assessment and Diffusion Tensor Imaging. *Neurology* **181,** 6–7 (2005).